

	ESA Contract:	1/6287/11/I-NB
		Doc. No:	D2100 Preliminary Analysis Report –draft
		Issue: 1	Date: 25.04.14

**CRYosat-2 sUCCess over Inland water And Land (CRUCIAL) Contract
1/6287/11/I-NB**

D2100 Preliminary Analysis Report

DRAFT

		ESA Contract:	1/6287/11/I-NB
		Doc. No:	D2100 Preliminary Analysis Report –draft
		Issue: 1	Date: 25.04.14

Document No: **NCL_CRUCIAL_D2100**

Issue: **1**

Issue Date: **25 April 2014**

Author: Steve Birkinshaw



Signature: *signed on original*

Author: Philip Moore

Signature: *signed on original*



Authorised by: Philip Moore

Signature: *signed on original*

		ESA Contract:	1/6287/11/I-NB
		Doc. No:	D2100 Preliminary Analysis Report –draft
		Issue: 1	Date: 25.04.14

Document Change Record

Version	Date	Modified by	Description
1	25.04.14	PM & SJB	Created

		ESA Contract:	1/6287/11/I-NB
		Doc. No:	D2100 Preliminary Analysis Report –draft
		Issue: 1	Date: 25.04.14

Abstract



Objectives:

The objective of WP2000 is to perform a comprehensive state-of-the-art review of all current initiatives, algorithms, models and EO based datasets relevant to the theme of Land and Inland water.

The review will include:

- A detailed review, assessment and cross-comparison of existing products, datasets, methods, models and algorithms, as well as related range of validity limitations, drawbacks and challenges.
- A detailed analysis of the suitable models and data integration approaches as well as their related limitations, drawbacks and challenges.
- A survey of all accessible associated data sets (space, airborne and in situ) which could be of use for development and validation activities (problems such as the lack of sufficient data sets will be investigated and practical solutions identified).
- An analysis and identification of the best candidate test areas to be used in later Work Packages. This shall include a complete analysis and description of the available data over those test areas.
- This will be obtained by performing a thorough review of the most current scientific publications in conjunction with drawing on the expertise of the consortium in related ESA projects, and other relevant research activities.



This document presents a Preliminary Analysis Report (PAR) resulting from the comprehensive state-of-the-art review of all current initiatives, models and the datasets relevant to the theme of Land and Inland water. It is one of two deliverables within Work Package 2000 (WP 2000) of

		ESA Contract:	1/6287/11/I-NB
		Doc. No:	D2100 Preliminary Analysis Report –draft
		Issue: 1	Date: 25.04.14

the CRUCIAL project; the other deliverable is the Development and Validation Plan (DVP).



The PAR document aims to:

- Produce a summary of the state of the art in waveform analysis and retracking, showcasing the technical state of the art and requirements over ocean, inland water and land surfaces.
- Presents the land specific state of the art overview, and outlines the proposed work to assess the land mapping contribution from Cryosat-2, including contributions to Global Digital Elevation Models (GDEM's).
- Presents the state of the art review for inland water and summarizes the proposed analysis of Cryosat-2 data, including the contribution from the river modelers, and gives a first identification of validation river basins.



		ESA Contract:	1/6287/11/I-NB
		Doc. No:	D2100 Preliminary Analysis Report –draft
		Issue: 1	Date: 25.04.14

Contents



1. Introduction	18
2. Cryosat-2	20
2.1 Cryosat-2 LRM Mode	22
2.2 Cryosat-2 SAR Mode: FBR and L1B	23
2.2.1 Previous Experience: ENVISAT and CRYMPS.....	24
2.2.2 L1A to L1B Processing.....	25
2.2.3 SAR Retrackerers	27
2.2.4 BEST Expert System	30
2.3 Cryosat-2 SARIN Mode.....	32
2.4 Cryosat-2 Improved corrections.....	35
2.4.1 Orbits	35
2.4.2 Troposphere Correction: Dry	35
2.4.3 Troposphere Correction: Wet.....	36
2.4.4 Ionosphere Correction.....	40
3. Land Surface Altimetry	44
3.1 DEM data and its Uses	44
3.2 SRTM and ASTER	45
3.3 ACE2.....	46

		ESA Contract:	1/6287/11/I-NB
		Doc. No:	D2100 Preliminary Analysis Report –draft
		Issue: 1	Date: 25.04.14

3.4	Earth2012 - Spherical harmonic models of Earth's topography and potential.....	48
4.	Inland Water.....	50
4.1	Satellite altimetry	50
4.1.1	Introduction	50
4.1.2	Rivers and Lakes project	51
4.1.3	Improvements suggested from Deliverable 1100.....	55
4.2	Repeat orbits and drifting orbits: implications for hydrological applications.....	56
4.3	Rivers	60
4.3.1	In-situ measured discharge data.....	61
4.3.2	Stage-discharge relationship.....	62
4.3.3	Hydrological modeling.....	66
4.3.4	River Uses 1 - Large and Poorly gauged river basins	67
4.3.5	River Uses 2 - Flood Dynamics and River-floodplain interactions.....	70
4.3.6	River Uses 3: Continental-scale water balance monitoring.....	71
4.4	Lakes	72
4.4.1	In-situ and satellite altimetry Water Level data.....	72
4.4.2	Lakes Uses 2: Long-term water level trends.....	76
4.4.3	Lakes Uses 2: Large ensembles of small water bodies.....	77
5.	Conclusions and Recommendations.....	79

		ESA Contract:	1/6287/11/I-NB
		Doc. No:	D2100 Preliminary Analysis Report –draft
		Issue: 1	Date: 25.04.14

6. References.....81

		ESA Contract:	1/6287/11/I-NB
		Doc. No:	D2100 Preliminary Analysis Report –draft
		Issue: 1	Date: 25.04.14

Figures

Figure 1 LRM Locations of successfully acquired waveform data from Cryosat-2 in period 2011/05/04 to 2011/06/01	22
Figure 2 Amazon waveforms: (Upper left) large number of spikes; (Upper right) oceanlike, (Lower left) oceanlike with second peak, (lower right) single spike.....	32
Figure 3 Difference between LRM (a) and SARIN (b) measurements in the optimal interpolation for common profiles of cross-track slope (c) and sea surface heights (d). The SARIN measurement allows observations of the cross-track slope in addition to the sea surface height profile given by the LRM mode (from Dibarboure et al. 2013)	34
Figure 4 IGS network: March 2014	37
Figure 5 Seasonal frequencies of cloud-free conditions across the globe during the period from March 2000 to February 2006. (a) Boreal spring (March–May); (b) boreal summer (June–August); (c) boreal autumn (September–November); (d) boreal winter (December–February).....	39
Figure 6 Differences between EIGEN-6C2 and EGM08. Taken from Forste et al (2012). Scale from -0.6 to +0.6 m.	43
Figure 7 ACE2 merged with Bathymetry	47
Figure 8 Geocentric distances to Earth Surface.....	49
Figure 9 River and Lake global locations	52
Figure 10 Satellite altimetry crossings and the near-by measured in-situ data for the Mekong river.....	54
Figure 11 ENVISAT and ERS-2 virtual stations on the Brahmaputra River	58



		ESA Contract:	1/6287/11/I-NB
		Doc. No:	D2100 Preliminary Analysis Report –draft
		Issue: 1	Date: 25.04.14

Figure 12 Cryosat-2 orbits over the Brahmaputra River. Red orbits belong to a first sub-cycle and blue orbits to a second sub-cycle. Numbers indicate relative overpass times in days..... 59

Figure 13 ADCP cross section of the Zambezi River 63



Figure 14 Cross-section method to measure river discharge (from Chow et al., 1988). 64

Figure 15 Example of a rating curve describing the relationship between water level and discharge 65

Figure 16 Major river basins of the world. Hydrological model development and use of radar altimetry (adapted from Bauer-Gottwein et al., 2013). 69



Figure 17 Map of the existing lakes and reservoirs of the HYDROWEB database..... 74

Figure 18 Map of the existing lakes and reservoirs of the USDA database..... 75

		ESA Contract:	1/6287/11/I-NB
		Doc. No:	D2100 Preliminary Analysis Report –draft
		Issue: 1	Date: 25.04.14



Tables

Table 1 Main characteristics of in-situ datasets and hydrological datasets derived from radar altimetry.....	66
Table 2 User requirements for the large and poorly-gauged river basins use case.	68
Table 3 User requirements for river-floodplain interaction use case	71
Table 4 User requirements for continental-scale water balance monitoring use.	72
Table 5 User requirements for the long-term water level trends use case	77
Table 6 User requirements for the large ensembles of small water bodies use	78



		ESA Contract:	1/6287/11/I-NB
		Doc. No:	D2100 Preliminary Analysis Report –draft
		Issue: 1	Date: 25.04.14

Abbreviations and Acronyms



Abbreviation	Meaning
ACE2	Altimeter corrected elevations 2 (digital elevation model)
ADCP	Acoustic Doppler Current Profiling
AIR	Azimuth Impulse Response
AMSR	Advanced Microwave Scanning Radiometer
ASCII	American Standard Code for Information Interchange – text file
ASTER	Advanced Spaceborne Thermal Emission and Reflection Radiometer
BEST	Berry Expert SysTem
CGIAR	Consultative Group on International Agricultural Research
CLS	Collecte Localisation Satellites
CNES	Centre National d’Etudes Spatiales
CP40	ESA Cryosat Plus for Oceans project
CRUCIAL	Cryosat-2 sUccess over Inland water And Land
CRYMPS	CryoSat Mission Performance Simulator
CRYPTIC	Cryosat Processing Transformation and Ingestion Code

		ESA Contract:	1/6287/11/I-NB
		Doc. No:	D2100 Preliminary Analysis Report –draft
		Issue: 1	Date: 25.04.14



CSI	Consortium for Spatial Information
DEMS	Digital Elevation models
DMU	De Montfort University
DORIS	Doppler Orbitography and Radiopositioning Integrated by Satellite - Doppler tracking and ground based satellite laser ranging
DTU	Danish Technical University
DVP	Development and Validation Plan
EAPRS	Earth and Planetary Remote Sensing Laboratory at DMU
ECMWF	European Centre for Medium-Range Weather Forecast
EGM08	Earth Gravitational Model 2008
EO	Earth Observatory
ENVISAT	Environmental Satellite
ERA	ECMWF ReAnalysis
ERS2	European remote sensing satellite 2
ESA	European Space Agency
ESRIN	European Space Research Institute
ETOPO1	Earth TOPOgraphy - 1 arc-minute global relief model of Earth's surface that integrates land topography and ocean bathymetry
FBR	Full Bit Rate

		ESA Contract:	1/6287/11/I-NB
		Doc. No:	D2100 Preliminary Analysis Report –draft
		Issue: 1	Date: 25.04.14



FFT	Fast Fourier Transform
GDEMS	Global Digital Elevation models
GDR	Geophysical Data Record
GEOTIFF	GEOfereced Tagged image File Format
GFO	Geosat Follow-On
GIM	Global Ionosphere Model
GLDAS	Global Land Data Assimilation System
GNSS	Global Navigation Satellite System
GOCE	Gravity field and steady-state Ocean Circulation Explorer – ESA satellite
GRACE	Gravity Recovery and Climate Experiment – NASA satellite
GRDC	Global Runoff Data Centre
GRS80	Geodetic Reference System 1980
HEC-RAS	Hydrologic Engineering Centers - River Analysis System
HYDROLARE	Hydrology of Lakes and Reservoirs
INSAR	Interferometric Synthetic Aperture Radar
IPF	Instrument Processing Facility
IRI	International Reference Ionosphere

		ESA Contract:	1/6287/11/I-NB
		Doc. No:	D2100 Preliminary Analysis Report –draft
		Issue: 1	Date: 25.04.14



Jason	US/French Altimeter Satellite
JPL	Jet Propulsion Laboratory
KO	Kick off
LIA	Level 1A
L1B	Level 1B
LEGOS	Laboratoire d'Etudes en Géophysique et Océanographie Spatiale
LRM	Low resolution Mode
MERIS	MEDium Resolution Imaging Spectrometer
METI	Ministry of Economy, Trade, and Industry – Japanese ministry
MODIS	Moderate Resolution Imaging Spectroradiometer
MWR	Micro-Wave Radiometer
NASA	National Aeronautics and Space Administration – US agency
NCEP	National Centers for Environmental Prediction – US agency
NCL	Newcastle University
NGA	U.S. National Geospatial-Intelligence Agency
NOAA	National Oceanic and Atmospheric Administration
NWM	Numerical Weather Model
OCO2	Offset Centre of Gravity

		ESA Contract:	1/6287/11/I-NB
		Doc. No:	D2100 Preliminary Analysis Report –draft
		Issue: 1	Date: 25.04.14

PAR	Preliminary Analysis Report
PLRM	Pseudo-LRM
POE	Precise Orbital Ephemeris
RA	Radar Altimeter
RDSAR	ReDuced Synthetic Aperture Radar
ROSHYDROMET	Russian Federal Service for Hydrometeorology and Environmental Monitoring
RIR	Range Impulse Response
RMS	Root Mean Square error
SAMOSa	Development of SAR Altimetry Studies and Applications over Ocean, Coastal zones and Inland waters
SAR	Synthetic Aperture Radar mode of Cryosat SIRAL
SARIN	Interferometric Synthetic Aperture Radar mode of Cryosat SIRAL
SENTINEL-3	ESA Earth Observation satellite mission
SEVIRI	Spinning Enhanced Visible and Infrared Imager
SIRAL	SAR Interferometric Radar Altimeter
SLR	Satellite Laser Ranging
SMMR	Scanning Multichannel Microwave Radiometer
SSM/I	Special Sensor Microwave/Imager

		ESA Contract:	1/6287/11/I-NB
		Doc. No:	D2100 Preliminary Analysis Report –draft
		Issue: 1	Date: 25.04.14

SRTM	Shuttle Radar Topography Mission
SWOT	Surface Water Ocean Topography Mission
TOPEX/Poseidon	US/French Altimeter Satellite (1992-2006)
TRMM	Tropical Rainfall Measuring Mission
VIC	Variable Infiltration Capacity hydrological model
VNIR	Visible and Near-InfraRed
WGHM	WaterGAP Global Hydrology Model
WGS84	World Geodetic System 1984
WMO	World Meteorological Organization
WP	Work Package
WTC	Wet troposphere correction

		ESA Contract:	1/6287/11/I-NB
		Doc. No:	D2100 Preliminary Analysis Report –draft
		Issue: 1	Date: 25.04.14

1. Introduction



This Deliverable 2100 (D2100) is part of work Package 2000 (WP 2000). The other deliverable in WP 2000 is the Development and validation plan – Deliverable 2200 (D2200).

This document contains a state-of-the-art review of all current initiatives under the theme of Land and Inland Water applications. This theme has two primary sub-themes; land surface height mapping and inland water monitoring. As the requirements and approach for these objectives contain both common and diverse elements, those aspects, which are application specific, are dealt with under separate specified headings. A Summary of work over the ocean is available from the preliminary analysis report carried out for ESA Cryosat Plus for Oceans (CP4O) project (Cotton et al. 2013; <http://www.satoc.eu/projects/CP4O/docs/CP4O-D21-PAR-V5c.pdf>). Much of the detail in that document is pertinent to inland and land applications and will not be repeated here. Rather we look at the distinction between ocean/coastal applications and those over land/inland waters.



Section 2 contains a summary of the state of the art in waveform analysis and retracking, including results from the SAMOSA project showcasing the technical state of the art and requirements over both inland water and land surfaces. A discussion of constraints is included.

Section 3 presents the land specific state of the art overview. The proposed work to assess the land mapping contribution from Cryosat-2, including contributions to Global Digital Elevation Models (GDEM's) are set out in the Development and Validation plan – Deliverable 2200 (D2200).

Section 4 presents the state of the art review for inland water including both rivers and lakes. The proposed analysis of Cryosat-2 data, including the contribution from the river modelers, and identification of validation river basins are set out in the D2200.

		ESA Contract:	1/6287/11/I-NB
		Doc. No:	D2100 Preliminary Analysis Report –draft
		Issue: 1	Date: 25.04.14



Section 5 presents the conclusions and recommendations.

		ESA Contract:	1/6287/11/I-NB
		Doc. No:	D2100 Preliminary Analysis Report –draft
		Issue: 1	Date: 25.04.14

2. Cryosat-2

Cryosat-2 was launched on 8 April 2010 into an orbit of 92° inclination and altitude 717 km. It follows on from previous earth orbiting satellite radar altimeters (e.g. ERS2 and ENVISAT) that have been used for land surface applications including mapping (Berry et al., 2010a; Smith and Berry, 2011) and measurement of river and lake systems (Berry et al., 2009a; Wheeler et al., 2010). Cryosat-2's primary instrument is SIRAL (SAR / Interferometric Radar Altimeter), which uses radar to determine and monitor the spacecraft's altitude. Although the primary aim of Cryosat-2 is to measure sea ice and ice sheets it can provide valuable data over the rest of the earth surface. SIRAL operates in one of three modes; depending on where (above the Earth's surface) Cryosat-2 is flying.



The three modes are: the conventional altimeter or Low resolution Mode (LRM), Synthetic Aperture Radar (SAR) and Interferometric Synthetic Aperture Radar (SARIN) with autonomous switching between modes based on a geographic mode mask (ESA 2013). CryoSat-2 has a low-earth orbit and is not Sun-synchronous; it has a period of 100 minutes. The Cryosat-2 mission is the first to operate a SAR mode Altimeter. Cryosat-2 is predominantly in the LRM mode. The LRM is the mode used by all previous altimetric missions namely a conventional pulse-limited radar altimeter. LRM, used over most land areas and over all ice-free ocean surfaces, requires a low-data bandwidth. The SAR mode operates over some land areas and ocean areas where sea-ice is prevalent. Both LRM and SAR modes utilise a transmission of identical pulses at a 13.575GHz. The main difference is the Pulse Repetition Frequency (PRF). In the LRM, the relatively low PRF implies that subsequent echoes are not correlated, and incoherent averaging can be used reducing noise. The LRM pulses are transmitted continuously. In the SAR mode, correlation between successive pulses facilitates coherent processing: this correlation is achieved using a relatively high PRF. The SAR mode pulses are emitted in a burst of 11.8 ms separated by 55 μ s (Galín et al. 2013). The returned echoes are processed coherently in the along-track direction forming a 26-m long synthetic aperture giving a narrow beam-limited foot

		ESA Contract:	1/6287/11/I-NB
		Doc. No:	D2100 Preliminary Analysis Report –draft
		Issue: 1	Date: 25.04.14

print 0.29 km in the along-track direction and pulse-limited and 1.5–3 km across-track direction (Raney, 1998). The echoes are sorted by Doppler frequency, giving rise to distinct radar-illuminated beams along the ground track described by the angle from the Earthward pointing nadir direction. Signals from multiple beams can be combined in a process called multilooking (Wingham et al. 2004) utilising range migration. In SARIN mode pulses are transmitted in burst (64 pulses per burst). The SARIN mode is designed to measure heights over land and ice-surfaces where there is significant cross-track slope such as at the ice sheet margins around the shorelines coastlines of Antarctica, Greenland and northern Canada. SARIN utilizes the two antennas on CryoSat-2 to form a cross-track interferometer with the echoes at each altimeter processed as in SAR mode (i.e. Doppler beam) but now with averaging over a lower number of waveforms averaged as the time interval between SARIN bursts is 47.17 ms.

Unlike LRM, SAR and SARIN require a very high bandwidth for downlinking. Although designed for ice and ice margins, data in SAR and SARIN mode have been collected over the oceans (Galini et al. 2013) for studies into mesoscale variability (Dibarboure et al. 2012) and the short-wavelength geoid (Stenseng and Andersen, 2012). The SAR mode is about a factor of two more accurate than the LRM but within the hardware design echoes from a burst are received at the satellite before transmission of the subsequent burst. This performance leads to a reduced data stream of 30%. Further details of SIRAL are given in the Cryosat-2 Product Handbook (ESRIN 2013).

The CRUCIAL project is investigating innovative land and water applications from Cryosat-2 with a forward-look component to the future Sentinel-3 mission. It is investigating the improvements that SAR mode altimetry can offer in measurements over land and inland water surfaces. It is very important to choose the best available processing methodologies, together with the best corrections and models. The project will provide a practical implementation of new theoretical models for the SAR echo waveform as part of this process.

		ESA Contract:	1/6287/11/I-NB
		Doc. No:	D2100 Preliminary Analysis Report –draft
		Issue: 1	Date: 25.04.14

Given that the LRM and SAR modes are mutually exclusive, the only possibility to compare the two modes is to reduce the high-PRF SAR echoes to the low-PRF LRM. The main difference between the LRM and SAR modes is the Doppler processing, which is the basis of any synthetic aperture approach. In CP40, three reduced SAR (RDSAR) techniques, independently developed and implemented by different groups were described. In RDSAR methodologies, SAR FBR echoes are combined coherently and/or incoherently in such a way that SAR PRF is effectively reduced from 17.8 KHz to a value close to the LRM PRF (1970Hz). SAR FBR data corresponds to individual complex (I and Q) components.

2.1 Cryosat-2 LRM Mode

Figure 1 shows the LRM is available over most of the earth surface.

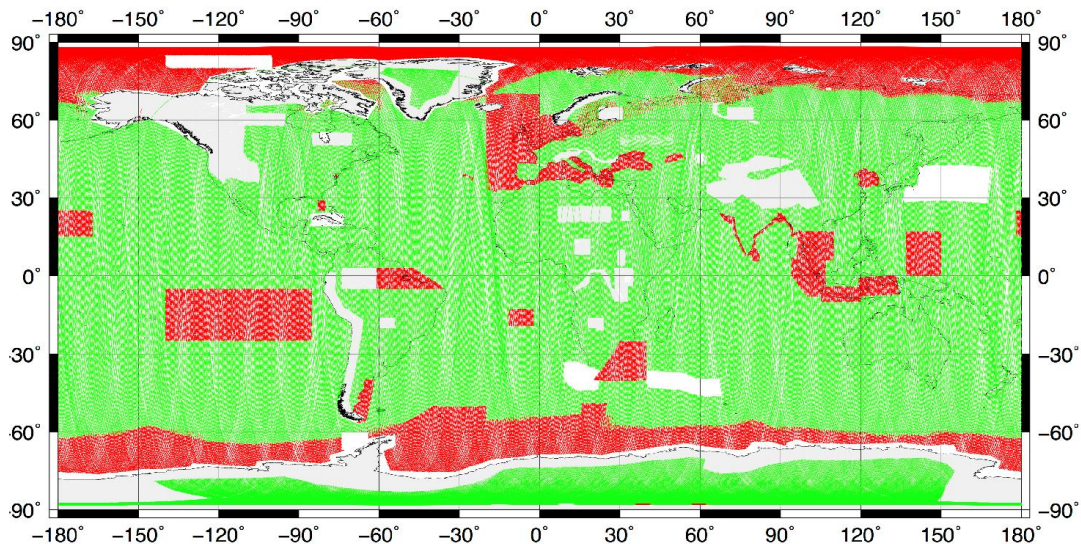




Figure 1 LRM Locations (Green) of successfully acquired waveform data from Cryosat-2 in period 2011/05/04 to 2011/06/01. SAR data is shown in red and SARIN is white.



		ESA Contract:	1/6287/11/I-NB
		Doc. No:	D2100 Preliminary Analysis Report –draft
		Issue: 1	Date: 25.04.14

The overall conclusion from initial analysis is that useable waveforms are being provided in LRM from Cryosat-2, and that a rough generic estimate would be that perhaps half of the records contain useable data over flat to moderate terrain. These waveforms have recognizable characteristics which can be related to the terrain overflown. This is extremely promising, and confirms that successful height retrieval over both land and inland water targets is possible from Cryosat-2 LRM waveforms. As for all altimeters, retracking the LRM data over land will require ingestion of sufficient data to enable parameter tuning of existing algorithms specific to the hardware and antennae properties of Cryosat-2.

2.2 Cryosat-2 SAR Mode: FBR and L1B

The CryoSat-2 SAR FBR and L1B are generated by the ESA Instrument processing Facility (IPF) and are often called the “Kiruna” products. It is these products that are distributed to users by ESA. The Full Bit Rate (FBR) product is the output of uncalibrated individual echoes after deramping in the time domain. The data consists of 128 bins of complex data (I and Q) for each of the 64 echoes in a pulse. Thus, the FBR data for SAR and SARIN modes contain the echo data as complex numbers. This data is also called the Level 1A (L1A) and is processed to form the L1B data. This is the lowest processing stage before information compression occurs.

Details on the SAR processing strategy from telemetered L1A data, to Level 1B and Level 2 are given in Wingham et al., (2006) and Dinardo (2013). The Level 1B (L1B) data is the main product output from the IPF1. In the case of SAR and SARIN modes of SIRAL, the L1B data are strongly compressed in size following the application of SAR/SARIN algorithms and multilooking for speckle reduction. Level 1B data consists of multi-looked echoes at a rate of, approximately, 20 Hz at each point along the ground track of the satellite.



		ESA Contract:	1/6287/11/I-NB
		Doc. No:	D2100 Preliminary Analysis Report –draft
		Issue: 1	Date: 25.04.14

CryoSat-2 SAR L1B products are currently available in Baseline B which replaced Baseline A in December 2012 due to the need to improve the performance of CryoSat-2 over sea ice. The next reprocessing (Baseline C) is expected mid-2014, will incorporate finer gate resolution and non-truncated waveforms (256 gates in SAR mode). Improvements over Baseline B include:

- correction for datation bias of approximately -0.5195 ms
- correction for a range bias of approximately -0.6730 m
- doubling of the waveform length in the Level 1B product with respect to Baseline B
- improved processing for 1Hz echoes to provide sharper waveforms
- surface sample stack weighting to filter out the single look echoes acquired at highest look angle, to give sharpened of 20Hz waveforms.

2.2.1 Previous Experience: ENVISAT and CRYMPS

Previous research with the ENVISAT Burst Echoes (Berry et al. 2007; Berry et al. 2009b; Witheridge et al., 2010, Berry et al, 2012) has shown that substantial high frequency information content is present at short spatial scales, because a small bright reflecting patch at nadir is able to dominate the returned echo. This effect is most strongly seen with inland water, because still water orthogonal to the incident pulse reflects the power back to the instrument (Berry et al., 2012). As water follows a surface of equal gravitational potential, it will always be approximately orthogonal to a nadir-pointing altimeter in a near-circular orbit. This means the onboard echo averaging of the current generation of satellite radar altimeters loses significant amounts of information. Thus when the Cryosat-2 altimeter is in SAR mode it offers the opportunity to recover high frequency signals over much of the Earth’s land surface, contributing to mapping applications, and transforming the inland water height retrieval capability. The main constraint

		ESA Contract:	1/6287/11/I-NB
		Doc. No:	D2100 Preliminary Analysis Report –draft
		Issue: 1	Date: 25.04.14



is the limited availability of SAR FBR data from Cryosat-2 (Figure 1); however, for Sentinel-3 the SAR mode will be deployed widely over land. It is worth pointing out that the scientific community has over 20 years of experience of using LRM altimetry whereas SAR altimetry is still in its infancy.

Previous SAR waveform analyses used results based on synthetic data from the CryoSat Mission Performance Simulator (CRYMPS). These showed the potential of SAR altimetry when compared to conventional altimetry. However, there have been problems encountered with the antenna mispointing angles on-board Cryosat-2 and this required several physically-based SAR waveform models to be developed within the ESA-funded SAMOSA “Development of SAR Altimetry Studies and Applications over Ocean, Coastal zones and Inland waters”. These include the SAMOSA2 (Ray et al. 2013) and the SAMOSA3 models (Gommenginger et al. 2012). Gommenginger et al. (2011) have looked at the performance of Cryosat-2 SAR mode data over the Norwegian Sea. They concluded that the L1B SAR oceanic and coastal waveforms are generally of a very high quality and that the SAMOSA models fit the Cryosat-2 waveforms over a wide range of sea-state conditions. Their latest retracker SAMOSA3 is able to capture the dominant aspects of the ocean and coastal SAR waveforms. The SAMOSA3 retracker is also to be used within the ESA eSurge project (Cipollini et al, 2013, <http://www.storm-surge.info/project>).

The CryoSat-2 studies to be carried out during this research will not only provide valuable data, but as precursors of the Sentinel-3 SAR mode data will give a valuable first look at this new measurement capability.



2.2.2 L1A to L1B Processing

Details processing strategy from Level 1A (L1A) to Level 1B (L1B) data is given in Wingham et al., (2006), Dinardo (2013) and CP40 (Cotton et al., 2013). In Wingham et al. (2006) expressions for the m^{th} echo within the 64 echo pulse following temporal Fast Fourier Transform (FFT) are

		ESA Contract:	1/6287/11/I-NB
		Doc. No:	D2100 Preliminary Analysis Report –draft
		Issue: 1	Date: 25.04.14

presented. It is assumed that calibration of the SAR waveforms has been undertaken prior to the formation and release of the L1A data. Beam formation follows by phase weighting and summing over all echoes in the pulse gives a new echo from the illumination of the one way power antennae pattern with the beam pattern. Processing restricts the look angle of the beam to a set of equal angular separations utilising the “rock angle” so that the beams of the next pulse coincident exactly with some of those of the previous pulse. Points that do not overlap define new ground points at which future bursts are directed. The number of equal angular separation (i.e. 64) enables use of the FFT. The process can also apply a weighting in the along-track direction to reduce the effects of side lobe ambiguities that appear as ghosting in the waveforms. A Hamming function is the usual suggestion for this task. The beam formulation using the rock angle applied to all Doppler beams is appropriate for surfaces that are level or with small undulations. More variable topography as for land use will need more precise steering. The beam formation will produce output from different pulses that illuminate the same ground location. The ground location viewed from different look angles are stacked and the Doppler beams in the stack corrected for differences in the slant range, to allow for change in the onboard tracker across all the beams and to allow for the Doppler shift in range due to the radar antennae motion during the pulse transmission. Range compression (using FFT) and multi-looking then give the L1B waveforms.

CP40 (Cotton et al., 2013) also review additional methodologies to process SAR Full Bit Rate (FBR data) to derive Low Resolution Mode (LRM) waveforms; the so-called ReDuced-SAR (RDSAR) techniques, and the resulting Pseudo-LRM (or PLRM) waveforms. Methodologies included the SAMOSA, CNES and NOAA/Altimetrics RDSAR methodologies. The motivation is to process SAR as a pseudo-LRM data compensating for PRF differences of the modes and associated effects (pulse-to pulse correlation or decorrelation). This is unnecessary for our applications as we are not seeking global uniformity in data.

		ESA Contract:	1/6287/11/I-NB
		Doc. No:	D2100 Preliminary Analysis Report –draft
		Issue: 1	Date: 25.04.14

2.2.3 SAR Retracker

This section presents a summary of the computations behind retracking of SAR waveforms. It is also to be emphasised that such retracker refer to L1B data unless specifically stated. A more comprehensive description is given in Cotton et al. (2013) for CP40. However, a brief summary is presented here as the formulation is necessary to understand how the different surfaces viewed (ocean, inland water, land) impact on the returned waveform and to differentiate between problems inherent with the reflecting surface. In SAR, as for standard LRM, the mean power of the waveforms $P(t)$ (Brown, 1977) can be formulated as a triple convolution of the response of the radar to a flat surface (P_{fs}), the point target response function (PTR) and the water/land surface elevation probability density function (PDF) specular points within the altimeter footprint, q_s

$$P(t) = P_{fs}(t) * q_s(t) * P_{PTR}(t) \quad (1)$$



where t is the time measured at the satellite receiver such that $t=0$ corresponds to the range to the mean sea level at nadir. SAR has a 2-dimensional PTR, the product of the range impulse response (RIR) and the azimuth impulse response (AIR) with the mean waveform a two-dimensional function of time (delay) and distance along-track (Doppler frequency). Brown (1977) showed that Eq. 1 can be written as

$$P(t) \approx P_{fs}(t) \int_0^{\infty} \int_{-\infty}^{\infty} \frac{c}{2} P_{PTR}(t-\tau) q_s\left(\frac{c}{2}(\tau-\hat{t})\right) d\tau d\hat{t} \quad (2)$$

where c is the speed of light. Ocean retracker for SAR mode are characterized by how the triple integral of Eq. 1 is evaluated.

i. Numerical Retracker

Numerical evaluation of the triple convolution gives an exact solution and is the method

		ESA Contract:	1/6287/11/I-NB
		Doc. No:	D2100 Preliminary Analysis Report –draft
		Issue: 1	Date: 25.04.14

adopted by CNES/CLS for example (e.g. Boy et al, 2012). The approach facilitates incorporation of forms of high complexity without approximation.



At CNES a Doppler waveform is fitted against a model generated offline. The offline model is parameterized by given instrumental and geophysical parameters. The requirement for modelled echoes can require extensive data storage and be computationally expensive if the echoes are sensitive to a large number of sea-state and altimeter hardware parameters. The off-line simulator computes families of models that equate to the SAR mode of Cryosat-2 through a number of stages including generation a flat sea-surface with high-resolution 1mx1m; the power return simulation in which the radar equation is applied at each point of the surface to compute the backscatter power taking into account the real elliptical antenna pattern after which the returns are sorted by Doppler band and accumulated in the appropriate range gates of the waveforms; while the flat sea-surface response is convolved with the PTR's. Finally the range corrected Doppler is used to form the Doppler echo model for a flat sea surface. As for conventional altimetry, the ocean parameters estimated from the numerical retracking are given by

$$\theta_n = \theta_{n-1} - g(BB^T)^{-1} \Big|_{\theta_{n-1}} (BD) \Big|_{\theta_{n-1}} \quad (3)$$

where θ_n is the estimated parameter at iteration n ; B, D the partial derivatives and residuals matrix, and g is the loop gain. Thus partial derivatives computed offline for each modelled echo need to be available. The CLS differs to some extent from that of CNES. At CLS the numerical database for simulations combines the Doppler processing scheme and the multilooking stages.

ii. Semi-analytical waveforms

These approximate the convolution in Eq. 1 by a number of approximations that reduce the convolution to a semi-analytical form. This was first proposed by Wingham et al. (2004), summarized by Cotton et al. (2013).

		ESA Contract:	1/6287/11/I-NB
		Doc. No:	D2100 Preliminary Analysis Report –draft
		Issue: 1	Date: 25.04.14



iii. Fully-analytical waveforms

Three physically-based SAR waveform models were developed within the ESA-funded SAMOSA project (Cotton et al., 2010). Numerical and analytical models were developed, and tested against simulated SAR waveforms from the CRYMPS simulator and against measured waveforms as provided in the ESA CryoSat-2 L1B SAR products. The retracker SAMOSA2 is semi-analytical and allows for effects such as asymmetry of the antenna beam, Earth's ellipticity of the Earth, along-track and across-track mispointing and non-linear ocean surface statistics (Ray et al., 2013). SAMOSA3, a simplified form of SAMOSA2, obtained after neglecting the nonlinear ocean surface effects and some second-order terms, is fully analytical providing a simple solution to compute the two-dimensional delay-Doppler maps of the SAR echo power as a function of range, significant wave height and backscatter coefficient, while retaining the advanced features of SAMOSA2 (Gommenginger et al., 2012).

iv. Empirical waveforms

A simplified retracking has been used by Garcia et al. (2014). That study is concerned with recovering the along-track ocean surface slope by estimating the range from consecutive radar altimeter waveforms. For marine gravity the waveform model is less complex than is required for absolute ocean surface height determination and uses a Gaussian approximation for the point target response. Garcia et al. (2014) accordingly developed an analytic formula for the shape of the SAR waveforms under the ideal condition of small radar mispointing angle and the deficiencies through a comparison waveform model from SAMOSA.

Equation 1 shows the dependence of the waveform on the surface via p_{fs} . Over oceans the surface response is straightforward to model and the waveforms are thus relatively predictable in character. Complexity is introduced when the surface becomes non-oceanic. To simulate and replicate SAR waveforms over land/inland water the surface response needs to model reflection from land (including sandbanks, river/lake boundaries, islands), vegetation and surface moisture, the inland water target (including surface roughness) and other inland waters or



		ESA Contract:	1/6287/11/I-NB
		Doc. No:	D2100 Preliminary Analysis Report –draft
		Issue: 1	Date: 25.04.14

wetlands including irrigated fields that are illuminated by the SAR. Building on consortium experience with LRM from previous satellite missions points to an order of magnitude increase in complexity over the ocean response. In particular, ocean retracers such as SAMOSA3 are not applicable over inland waters etc. Composite waveform structure is likely to dominate SAR waveforms across even wide bodies of inland water and deconstruction of the waveform into its dominant constituents will be necessary. Examples of waveforms from Cryosat-2 SAR are given in Figure 2. The green line in the sub-figures show the Offset Centre of Gravity (OCOG) measurement reference point (MRP). The oceanlike is typical of an open ocean waveform. The oceanlike with a second peak that probably contains an off-river scattering but not clear which peak is the river, the waveform in the upper left is impossible to interpret. Other examples could have been used but these are representative of the complexity of interpretation over inland waters.

2.2.4 BEST Expert System



The Berry expert SysTem (BEST) utilized for previous altimeter missions and ongoing with Jason-2 is based around a number of retracers that are matched to the observed waveforms. BEST has been applied on a global scale after extensive research and analysis of land altimeter echoes from ERS-1, ERS-2 Ku band and EnviSat Ku and S band over the past seven years, complemented by an analysis of Topex data in both Ku and C bands, and both Jason1 and Jason2 Ku band data. The expertise garnered with BEST through participation in the SAMOSA contract, where input scenarios for the CRYMPS simulator were designed and the returned outputs analysed, gives the capability to process and analyse SAR Level1-B (L1B) and Low Resolution Mode (LRM) data.

Within BEST, in order to interpret the complex shapes returned from topographic surfaces, a

		ESA Contract:	1/6287/11/I-NB
		Doc. No:	D2100 Preliminary Analysis Report –draft
		Issue: 1	Date: 25.04.14

rule based expert system has been developed. This system can be used for echo analysis, to generate retracked heights and assess new retracker performance, and to generate reference and comparison data. As for any new altimeter mission the retracker will need tuning for the specific characterisation of the Cryosat-2 hardware. With respect to SAR waveforms several of the retracker classes will be applicable after tuning (based on global analysis) building on the experience with CRYPTIC (Cryosat Processing Transformation and Ingestion Code). CRYPTIC allowed automated processing of the SAR FBR and LRM data by reading the CryoSat-2 data into predefined structures using the C programming language. These structures can then be used to modify the data as necessary to provide compatibility with various processing algorithms.

As seen in Figure 1, CryoSat-2 is in SAR mode over a very limited part of the Earth’s land surface. Initial analysis of the data with BEST with L1B data has been carried out as part of WP4000 as it has been observed that the full sequence across an inland water body includes a number of highly complex waveforms, some of which were successfully accepted by the dedicated retracking algorithms in the BEST. Some unusual features (Fig. 2) are apparent in the waveform sequences, which must be investigated further. Detailed investigation of such waveforms over inland water and topographic surfaces, and validation with independent data, need further study, in order to define optimal retracker for SAR waveforms for land and inland water waveforms; currently the scope of this analysis is limited to some extent by the small quantities of land SAR mode data and correspondingly SAR FBR waveforms. One key investigation for the first part of the CRUCIAL work is thus the determination of what parts of target river basin (Deliverable D2200) return echoes are successfully captured by the altimeter. Consideration also needs to be given to L1A data both to develop a “L1B – like” processing stream for inland water and as a forward look to the Sentinel-3 mission for which L1A data will be the norm.

		ESA Contract:	1/6287/11/I-NB
		Doc. No:	D2100 Preliminary Analysis Report –draft
		Issue: 1	Date: 25.04.14

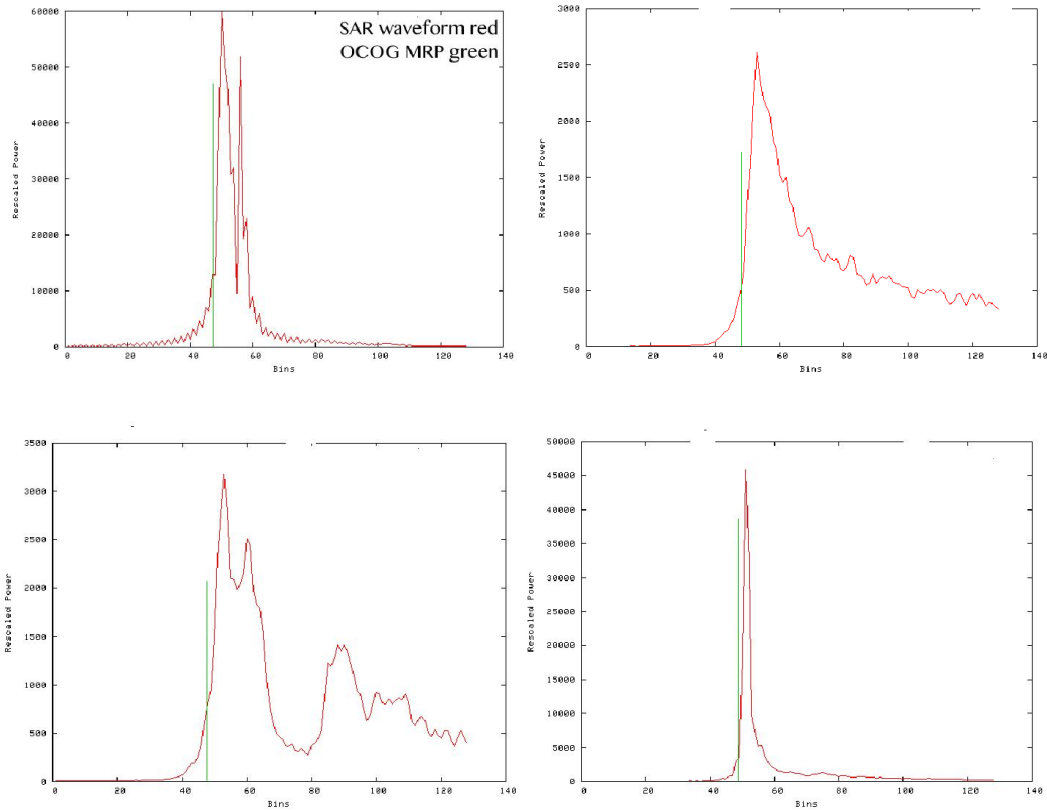




Figure 2 Amazon waveforms: (Upper left) large number of spikes; (Upper right) oceanlike, (Lower left) oceanlike with second peak, (lower right) single spike.

2.3 Cryosat-2 SARIN Mode



Interferometric Synthetic Aperture Radar (SARIN) is the third of the three modes for Cryosat-2, with autonomous switching between modes based on a geographic mode mask (ESA 2013). The

		ESA Contract:	1/6287/11/I-NB
		Doc. No:	D2100 Preliminary Analysis Report –draft
		Issue: 1	Date: 25.04.14

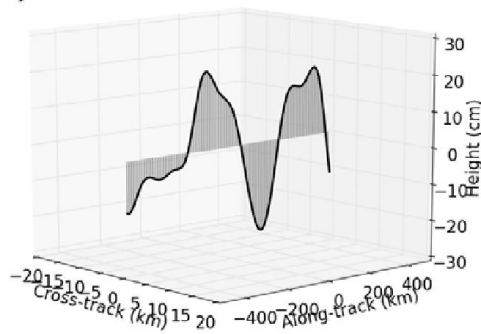
SARIN mode uses CryoSat-2's two antennas. The combination of SAR and interferometry makes it possible to determine the cross-track slope of the surface from which the echoes are arriving. This is achieved by comparing the phase of one receive channel with respect to the other. The echoes at each altimeter are processed as in SAR mode (i.e. Doppler beam) but now with averaging over a lower number of waveforms averaged as the time interval between SARIN bursts is 47.17 ms; this is in addition to the classical elevation measurements (Figure 3). Moreover, the along-track resolution and the precision of surface elevations is the same as for a LRM sensor. The resolution is 300 m in the along-track direction (synthetic footprint), and the slope is estimated from a cross-track footprint of the order of 7 km.

SARIN was initially designed to be used over the margins of the Greenland and Antarctic ice sheets, where the surface slopes are steep. To that extent, SIRAL's SARIN mode was designed to have a cross-track slope accuracy of 200 μ rad but Galin et al (2013) reported a noise level of 20 μ rad at a 7 km resolution and a bias of 8 μ rad for 1000 km segments, using both detailed modelling of the finite radar resolution in range and angle, and the thermally driven behaviour of the interferometer bench.

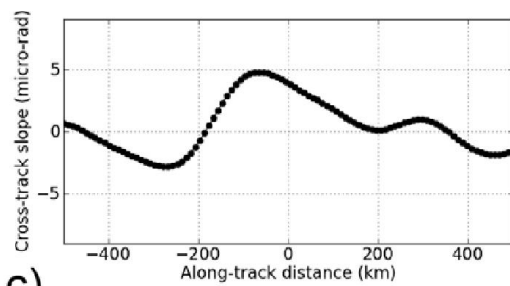
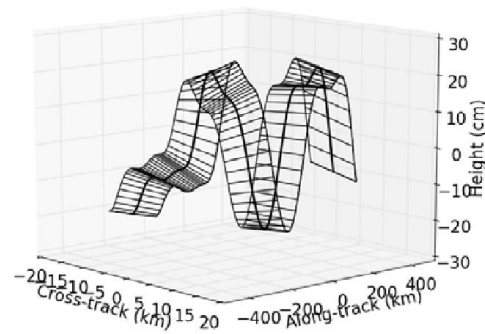
Dibarboure et al. (2013) have explored the potential of the cross-track slope derived from the Cryosat-2 SARIN mode over the oceans to increase the resolution of mesoscale fields in the cross-track direction.

		ESA Contract:	1/6287/11/I-NB
		Doc. No:	D2100 Preliminary Analysis Report –draft
		Issue: 1	Date: 25.04.14

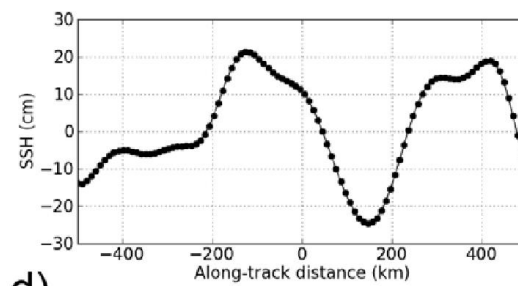
a) LRM sea surface height profile



b) SARin height & slope profile





c)



d)

Figure 3 Difference between LRM (a) and SARIN (b) measurements in the optimal interpolation for common profiles of cross-track slope (c) and sea surface heights (d). The SARIN measurement allows observations of the cross-track slope in addition to the sea surface height profile given by the LRM mode (from Dibarboure et al. 2013)

		ESA Contract:	1/6287/11/I-NB
		Doc. No:	D2100 Preliminary Analysis Report –draft
		Issue: 1	Date: 25.04.14



2.4 Cryosat-2 Improved corrections

Successful height recovery from retracked waveforms needs a number of orbital and geophysical parameters to be able to extract the inland water/land surface height relative to some datum such as the WGS84 or GRS80 ellipsoids. These include the orbital height derived from precise tracking of the satellite, and corrections that need to be applied to the altimetric height due to the atmosphere, ionosphere, and solid earth tides etc. Some corrections are easy to model accurately (e.g. solid earth tides) through standard algorithms and will not be considered further. Previous conventional altimeter missions included a microwave radiometer (MWR) for wet troposphere corrections and the ability to make measurements of the first order ionospheric effect by means of a dual frequency altimeter. This information is not available for Cryosat-2, and hence these corrections are discussed further in Sections 2.4.2 and 2.4.3. However, since the orthometric height requires an independent measure of the satellite height we start with discussion of the orbit in Section 2.4.1.

2.4.1 Orbits

Precision orbit determination of Cryosat-2 relies on DORIS Doppler tracking and ground based satellite laser ranging. With SLR RMS residuals of around 2 cm the orbits can be considered of Jason-2 class. Comparisons between the CNES Precise Orbital Ephemeris (POE) and independent orbits (Schrama et al., 2013) show an RMS agreement of 1.5 cm in the radial direction. Orbital accuracy is thus not a consideration over inland waters given the uncertainties elsewhere in the derived height formulation.

2.4.2 Troposphere Correction: Dry

		ESA Contract:	1/6287/11/I-NB
		Doc. No:	D2100 Preliminary Analysis Report –draft
		Issue: 1	Date: 25.04.14



The dry tropospheric, H_{dry} , in millimetres can be calculated from:

$$H_{dry} = -2.277 P (1 + 0.0026 \cos 2\phi + 0.00028h) \quad (4)$$

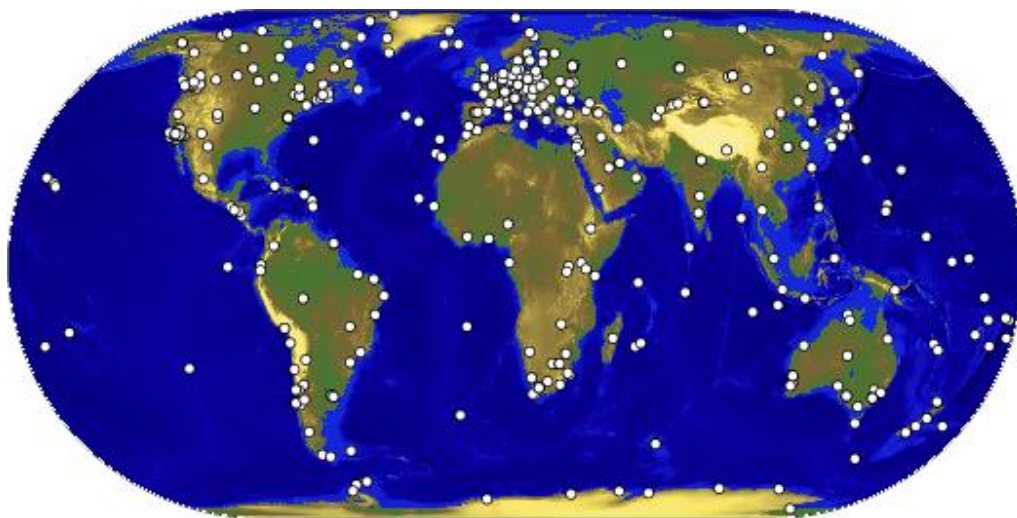
where P is surface atmospheric pressure (hPa), h the surface height above the geoid (m), and ϕ the latitude of the station. Surface pressure can be extracted from the ECMWF Numerical Weather Model (NWM). Salstein et al. (2008) compare NCEP and ECMWF analyses of surface pressure to an extensive set of surface barometric observations for the period 2001–2005. Over most land areas, typical error variances are below 1 hPa². Areas with high RMS values included high topographic regions such as the Tibetan Plateau, southern Africa, and South America, near the Andes. For the five calendar years 2001-5, the area-weighted RMS values are 2.51, 2.46, 2.39, 2.40 and 2.49 hPa respectively. As an error of 1 hPa equates to a dry tropospheric correction error of 2.3 mm; uncertainties in the dry tropospheric correction are thus generally less than 1 cm.

2.4.3 Troposphere Correction: Wet

The wet tropospheric correction with magnitude of up to 50cm is one of the major sources of error over land and inland waters. The wet tropospheric correction is highly variable spatially and temporally with strong altitude dependence. Previous altimeter missions carried a microwave radiometer (MWR) for measurement of the total water vapour content in the nadir direction over oceans: the MWR is swamped by temperature brightness from land and hence are inoperative over non-ocean surfaces. However, as CryoSat-2 is primarily dedicated to measuring and monitoring the changing thickness of ice in polar regions it was not equipped with a MWR. Rather the Cryosat-2 altimeter records will provide a correction from a NWM run by the ECMWF. Given the possibility of inaccuracy within the NWM, the ESA funded project CP40 “CryoSat Plus for Oceans” aims to provide an improved wet tropospheric correction over

		ESA Contract:	1/6287/11/I-NB
		Doc. No:	D2100 Preliminary Analysis Report –draft
		Issue: 1	Date: 25.04.14



the oceans based on a data combination algorithm of existing global-scale data types. Their approach based on Fernandes et al. (2013) is to fuse all available data from the ECMWF ReAnalysis (ERA) Interim model, GNSS total delay measurements at coastal sites and remote sensing data from water radiometers on other remote sensing satellites operational over the Cryosat-2 lifetime. For land and inland water applications over remote areas as in Africa, Asia and South America (see Figure 4) the distribution of GNSS stations is sparse or non-existent to the extent that a NWM or remote sensing satellites are the only viable source of data.



CSMT 2014 May 05 18:45:02



Figure 4 IGS network: March 2014

Remote sensing of water vapour offers the potential for global recovery of the wet tropospheric correction but they are usually limited in spatial and/or temporal coverage and resolution. Near infrared (NIR) and optical sensors such as the Medium Resolution Imaging Spectrometer (MERIS) onboard ENVISAT, the MODerate Resolution Imaging Spectroradiometer (MODIS) on the Terra and Aqua satellites and the Spinning Enhanced Visible and Infrared Imager (SEVIRI) of the Meteosat Second Generation satellite cannot see through clouds which severely limits

		ESA Contract:	1/6287/11/I-NB
		Doc. No:	D2100 Preliminary Analysis Report –draft
		Issue: 1	Date: 25.04.14

application over land. Furthermore, given the large spatial and temporal variation in the wet tropospheric correction an instrument onboard the altimeter satellite is ideally required to ensure contemporaneous measurements of altimetric height and water vapour. The latter is a severe limitation with analyses such as by Li et al. (2006, 2009) with MERIS indicating global cloud free conditions at the ~25% level although some areas such as Eastern Tibet (~38%) and Southern California (~48%) are much higher. A combination of sensors from different platforms such as MERIS and MODIS (e.g. Li et al., 2009) has potential to increase the cloud free occasions but a time difference will exist between the altimeter and MODIS measurements. Figure 5 from Li et al. (2009) shows the global seasonal frequencies of cloud-free conditions from March 2000 to Feb 2006. Clearly, there are seasons and regions where NIR sensors can be used for estimation of the wet tropospheric correction but conversely there are significant seasonal and regional constraints.

The adequacy of the ECMWF product will need consideration if the uncertainty in the wet tropospheric correction over land and inland waters warrants a detailed examination.

		ESA Contract:	1/6287/11/I-NB
		Doc. No:	D2100 Preliminary Analysis Report –draft
		Issue: 1	Date: 25.04.14

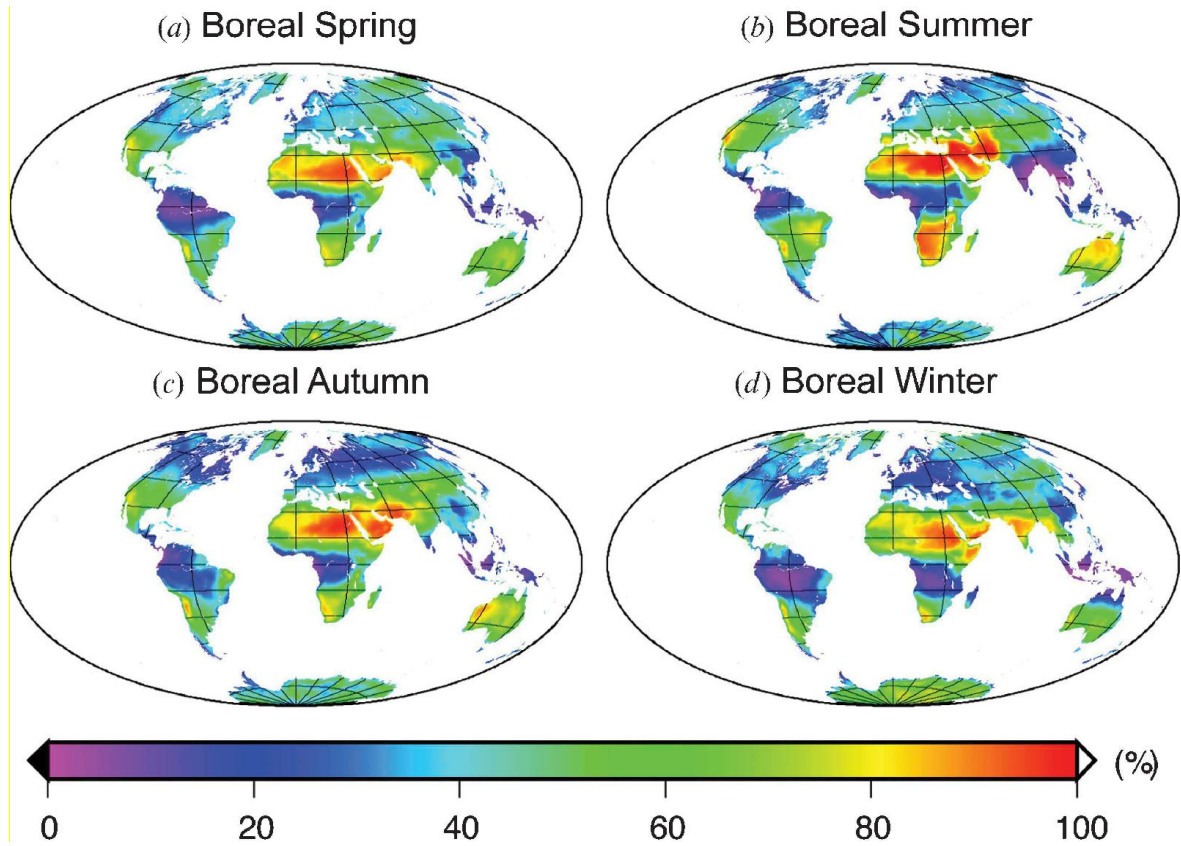




Figure 5 Seasonal frequencies of cloud-free conditions across the globe during the period from March 2000 to February 2006. (a) Boreal spring (March–May); (b) boreal summer (June–August); (c) boreal autumn (September–November); (d) boreal winter (December– February).

		ESA Contract:	1/6287/11/I-NB
		Doc. No:	D2100 Preliminary Analysis Report –draft
		Issue: 1	Date: 25.04.14



2.4.4 Ionosphere Correction

Previous altimetric satellites after ERS-1/2 carried dual frequency altimeters to eliminate the effect of the ionosphere (0.6-1.2 m) which to first order is a frequency dependent correction. For such altimetric missions the smoothed dual-frequency ionosphere correction is probably accurate to 5 mm. Cryosat-2 carries a single frequency altimeter (13.575 GHz; Ku band) and thus as for ERS is dependent on an external measure of the ionospheric correction. Available models include the JPL Global Ionosphere Model (GIM) and NIC08 (Scharroo, et al., 2008) both derived from the global GNSS network and the Bent model (Bent et al., 1972). Scharroo et al (2008) concluded that the models are probably close to the 5mm accuracy of the dual-frequency ionosphere correction during low solar activity but increase to about 2 cm global RMS during high solar radiation whilst models from DORIS and the International Reference Ionosphere IRI2007 (Bilitza and Reinisch, 2008) are at least a factor of 2 worse. The GIM ionospheric correction is the nominal model for Crosat2 with Bent as backup.

2.4.5 Geoid Model

Previous altimetric missions have tended to follow a particular ground track pattern that repeated after a number of days (~10 days for TOPEX/Poseidon, Jason-1, Jason2; 35 days ERS-1, ERS-1, ENVISAT). Thus, by differencing profile heights from a mean profile gave a time series of variability for hydrological inferences. However, Cryosat-2 is in a non-repeat orbit; the ground tracks do not repeat. For inland waters the implication is that the altimetric heights which act as a virtual gauge will not be at the same crossing of a river or profile across the lake. For lakes this is not a severe limitation as the lake surface will effectively lie on an equipotential surface of the Earth's gravity field and hence a geoid model can be used to connect different sub-satellite points and passes utilizing the relative geoid height between two points.



Geoid modelling across lakes requires a high resolution gravity field. If I_{\max} is the maximum

		ESA Contract:	1/6287/11/I-NB
		Doc. No:	D2100 Preliminary Analysis Report –draft
		Issue: 1	Date: 25.04.14

degree modelled then the shortest half-wavelength on the Earth’s surface given by the field is $20000/l_{\max}$ km. Gravity fields are estimated from orbital perturbations, satellite tracking, altimetry and terrestrial gravimetric data. Conventional satellite tracking using camera data, SLR and microwaves can provide the longer wavelengths of the gravity field to degree and order about 70 but are limited beyond that by the attenuation of the gravity field with height. For that reason dedicated gravity field missions were launched. These include the Gravity and Circulation Experiment (GRACE) and ESA’s Gravity and steady-state Ocean Circulation Explorer (GOCE) missions. GRACE is designed for temporal gravity field modelling although static models have been derived to degree and order 180. As with all gravity fields, accuracy of the coefficients decreases with the degree so that high accuracy is achieved at lower degrees than the stated maximum. GOCE has provided the highest accuracy intermediate gravity field harmonics say (180 – 250) to date. A combination model from GOCE, GRACE, satellite tracking, altimetry and gravimetry will provide the best field.

Given the objective of modelling equipotential surfaces on lakes only fields containing gravimetric data will give the required resolution. Available fields include EGM08 (Pavlis et al., 2012) a field complete to degree and order 2160 with some coefficients to degree and order 2190. EGM08 incorporates GRACE data but not GOCE. Other fields include the EIGEN series of models released by GFZ, Potsdam, and GRGS, Toulouse. EIGEN-6C (Shako et al. 2014) was the first combined gravity field model computed from LAGEOS, GRACE and GOCE data, augmented with the DTU10 surface gravity data and containing time variable parameters to degree/order 50. Enhancements to EIGEN-6C include EIGEN-6C2 (Förste et al. 2011). The next upgrade will be EIGEN-6C4 which will include the latest release of GOCE and GRACE data. Currently EIGEN-6C3stat, a static pre-version of EIGEN-6C4 to degree and order 1949, is available. Differences between EIGEN-6C4 and EGM08 at the short wavelengths are expected to be small as both depend on the gravimetric data. EIGEN-6C4 utilises DTU10 surface gravity which defaults to EGM08 over the land.



EGM08 geoid heights are available from U.S. National Geospatial-Intelligence Agency (NGA) on

		ESA Contract:	1/6287/11/I-NB
		Doc. No:	D2100 Preliminary Analysis Report –draft
		Issue: 1	Date: 25.04.14

regular grids of 1'x1' and 2.5'x2.5'. Alternatively, the geoid undulations can be determined by the user using NGA software, the EGM08 harmonic coefficients and a file to correct the height anomalies to a geoidal height. It is expected that EIGEN-6C4 will have similar downloads.

Analysis of EGM-08 and EIGEN fields over lakes need to be undertaken. Figure 6 shows that over a 0.25°x0.25° grid the differences between EIGEN-6C2 and EGM08 to degree and order 360 can reach near 0.6m. Differences beyond 360 are expected considerably larger in certain locations. With geoid heights available over inland water, differential geoid heights between locations will facilitate derivation of Cryosat-2 time series for non-repeat profiles.

This above process will differ from that adopted in the “Rivers and Lakes” project where the precursor EGM96 to EGM08 provided the geoid. However, the geoid was complemented through addition of a mean profile along the ground track using about 3 years of repeat pass data. This addition essentially gives the derivation of the true geoid from the modelled geoid along the track. In that way a single measurement in the time series of variability in lake level was computed by utilizing all measurements on the repeat pass. For Cryosat-2, it will not be possible to supplement the computed height with an altimetric correction given the non-repeat orbit and hence we will rely completely on the computed differential geoid heights.

		ESA Contract:	1/6287/11/I-NB
		Doc. No:	D2100 Preliminary Analysis Report –draft
		Issue: 1	Date: 25.04.14

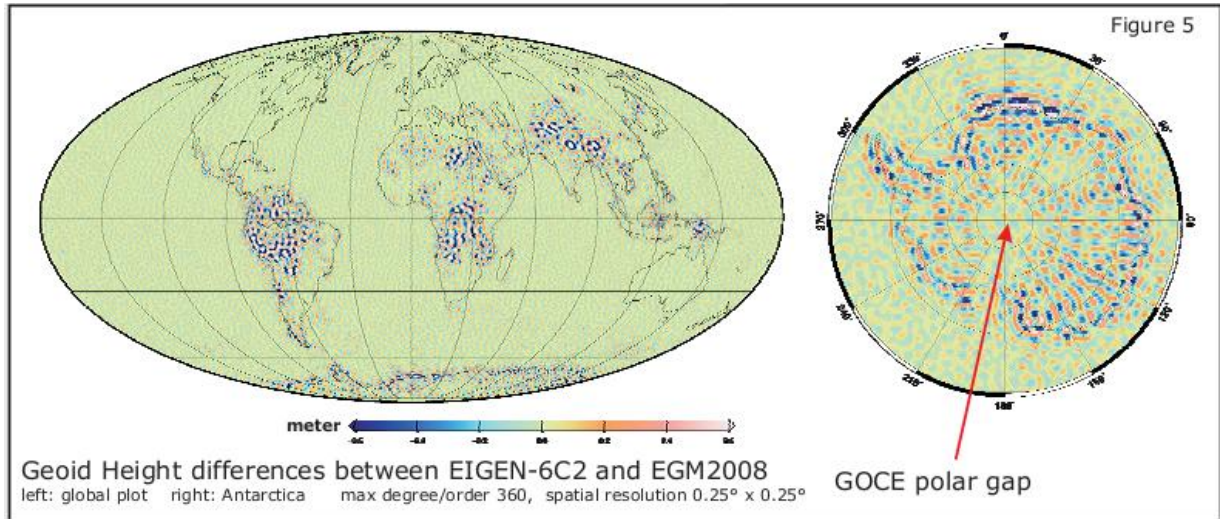




Figure 6 Differences between EIGEN-6C2 and EGM08. Taken from Forste et al (2012). Scale from -0.6 to +0.6 m.

		ESA Contract:	1/6287/11/I-NB
		Doc. No:	D2100 Preliminary Analysis Report –draft
		Issue: 1	Date: 25.04.14



3. Land Surface Altimetry

3.1 DEM data and its Uses

A digital elevation model (DEM) or Global digital elevation model (GDEM) is a digital model or 3D representation of a terrain's surface created from terrain elevation data. A DEM is often represented as a raster (a grid of squares). The DEM can be acquired through a variety of techniques but recently, in many cases, the data is collected using remote sensing techniques.

There are a large number of potential uses for DEM data and these have been reviewed by Zandbergen (2008). The freely available remote sensing DEMs (SRTM and ASTER, see section 3.2) have probably had the largest impact on studies of regions for which reliable, high-resolution digital topography was not previously available. But even for where high resolution DEM are available the remote sensing DEMs are being employed for hydrological modeling because it provides greater uniformity of quality and coverage and so enables more reliable comparison across boundaries between different countries. Examples of where remote sensed DEM data is used include:

- Forest ecology – tree height, density and structure
- Glaciology – glacier mass balance
- Volcanology – lava flows
- Geomorphology – unique features in remote regions
- Hydrology – extraction of drainage networks and upstream catchment areas
- Hydrology – rainfall runoff models
- Hydrology – surface water heights

		ESA Contract:	1/6287/11/I-NB
		Doc. No:	D2100 Preliminary Analysis Report –draft
		Issue: 1	Date: 25.04.14



- Coastal Flooding
- Urban development
- Archeology - identification of archaeological sites

3.2 SRTM and ASTER

The Shuttle Radar Topography Mission (SRTM) was an international research effort that obtained digital elevation models on a near-global scale from 56° S to 60° N. SRTM consisted of a specially modified radar system that flew on board the Space Shuttle Endeavour during the 11-day STS-99 mission in February 2000 (NASA JPL, 2011). To acquire topographic (elevation) data, the SRTM payload was outfitted with two radar antennas. One antenna was located in the Shuttle's payload bay, the other on the end of a 60-meter (200-foot) mast that extended from the payload bay once the Shuttle was in space. The technique employed is known as Interferometric Synthetic Aperture Radar (INSAR). The main problems with the dataset were voids and poor results over deserts, high mountains regions and water bodies. Also as SRTM data is derived from radar it represents the elevation of the first-reflected surface so, in particular, in forests it is not necessarily representative of the ground surface.

Groups of scientists have worked on algorithms to fill the voids of the original SRTM data. Two datasets offer global coverage void-filled SRTM data at 90m: the CGIAR-CSI versions (<http://srtm.csi.cgiar.org>) and the HydroSHEDS dataset (<http://hydrosheds.cr.usgs.gov/>). There have now been over 750,000 confirmed users of the CGIAR-CSI dataset. Data can be downloaded as an ASCII file or a GeoTiff.

ASTER (Advanced Spaceborne Thermal Emission and Reflection Radiometer) is a sensor produced by the The Ministry of Economy, Trade, and Industry (METI) of Japan which is one of

		ESA Contract:	1/6287/11/I-NB
		Doc. No:	D2100 Preliminary Analysis Report –draft
		Issue: 1	Date: 25.04.14



five remote sensory devices on board the Terra satellite launched into Earth orbit by NASA in 1999 (METI and ASTER 2011). The instrument has been collecting superficial data since February 2000. ASTER provides high-resolution images of the planet Earth in 14 different bands of the electromagnetic spectrum, ranging from visible to thermal infrared light. The ASTER DEM model covers the planet from 83 degrees North to 83 degrees South. It was created by compiling 1.3 million visible and near-infrared (VNIR) images taken by ASTER using single-pass stereoscopic correlation techniques, with terrain elevation measurements taken globally at 30 meter intervals. The 30m GDEM can be downloaded from <http://gdem.ersdac.jspacesystems.or.jp/>.

There have been a number of studies looking the accuracy of the DEM data from ASTER and SRTM. Mukherjee et al. (2013) have carried out a recent comparison for India and found the overall vertical accuracy shows RMS error of 12.62 m and 17.76 m for ASTER and SRTM DEM respectively.

In 2014, acquisitions from radar satellites TerraSAR-X and TanDEM-X will be available in the form of a uniform global coverage with a resolution of 12 meters.

3.3 ACE2

The ACE2 GDEM (Berry et al, 2010b) was created by the former EAPRS Lab at De Montfort University (DMU) and was the successor to the highly successful ACE GDEM. In ACE2 (Figure 7) high accuracy multi-mission satellite radar altimetry was fused with the high frequency content of the SRTM DEM (NASA JPL, 2011). Over 100 million height points derived from the Berry Expert SysTem (BEST) retracked altimeter data points were used to generate warping factors to bring the SRTM surface into agreement with the radar altimeter derived surface. This resulted in not only the most accurate GDEM to date but also led to the generation of a set of additional matrices, providing unique and useful information. Height data were produced at spatial

		ESA Contract:	1/6287/11/I-NB
		Doc. No:	D2100 Preliminary Analysis Report –draft
		Issue: 1	Date: 25.04.14

resolutions of 3", 9" merged with Mean Sea Surface, 30" and 5' merged with bathymetry. These matrices were the Source matrix denoting which datasets were used to create each pixel; the Quality matrix which provides an estimate of accuracy for each pixel and finally the Confidence matrix which details the confidence per pixel in the height and accuracy estimate provided by the Quality matrix. This rich additional data source allows users to make a fully informed decision when deciding how best to use the ACE2 GDEM.

For the 3" data there are 288 tiles each covering 15 degrees of latitude and 15 degrees of longitude. For all the data the height DEM is provided as 4 byte float data in a simple binary raster.

Chang et al. (2010) have carried out an assessment of ACE2 compared to SRTM and ASTER datasets.

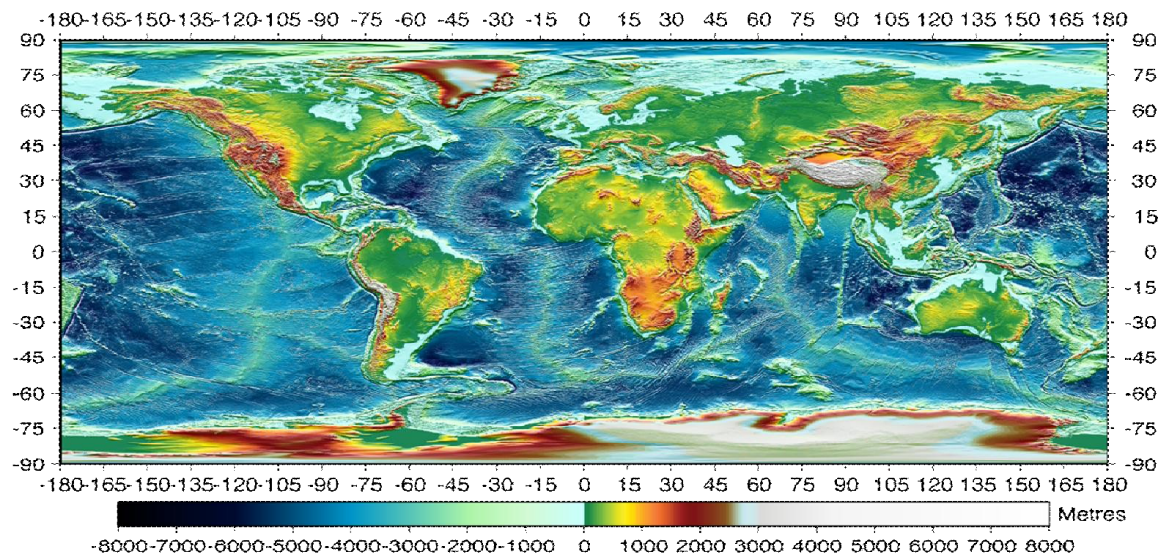




Figure 7 ACE2 merged with Bathymetry



		ESA Contract:	1/6287/11/I-NB
		Doc. No:	D2100 Preliminary Analysis Report –draft
		Issue: 1	Date: 25.04.14

3.4 Earth2012 - Spherical harmonic models of Earth's topography and potential

A recent topographic release (Hirt and Kuhn, 2012) gives a suite of spherical harmonic models of the Earth's topography, rock-equivalent topography, Earth's shape and implied topographic potential complete to degree and order 2160. The spherical harmonic models (Figure 8) are based on

- SRTM V4.1 hole-filled 250m resolution release by CGIAR-CSI Consortium for Spatial Information within the coverage of the Shuttle Radar Topography Mission,
- SRTM30_PLUS bathymetry (by University of California) over the oceans and major lakes
- NOAA's ETOPO1 ice and bed-rock data over Antarctica and Greenland.

The shape models (with water, without water, without water and ice, rock equivalent topography) give the geocentric distance to the surface point. The Earth2012 models were used in recent studies on GOCE gravity fields and Earth's topographic potential (Hirt et al., 2012).

		ESA Contract:	1/6287/11/I-NB
		Doc. No:	D2100 Preliminary Analysis Report –draft
		Issue: 1	Date: 25.04.14

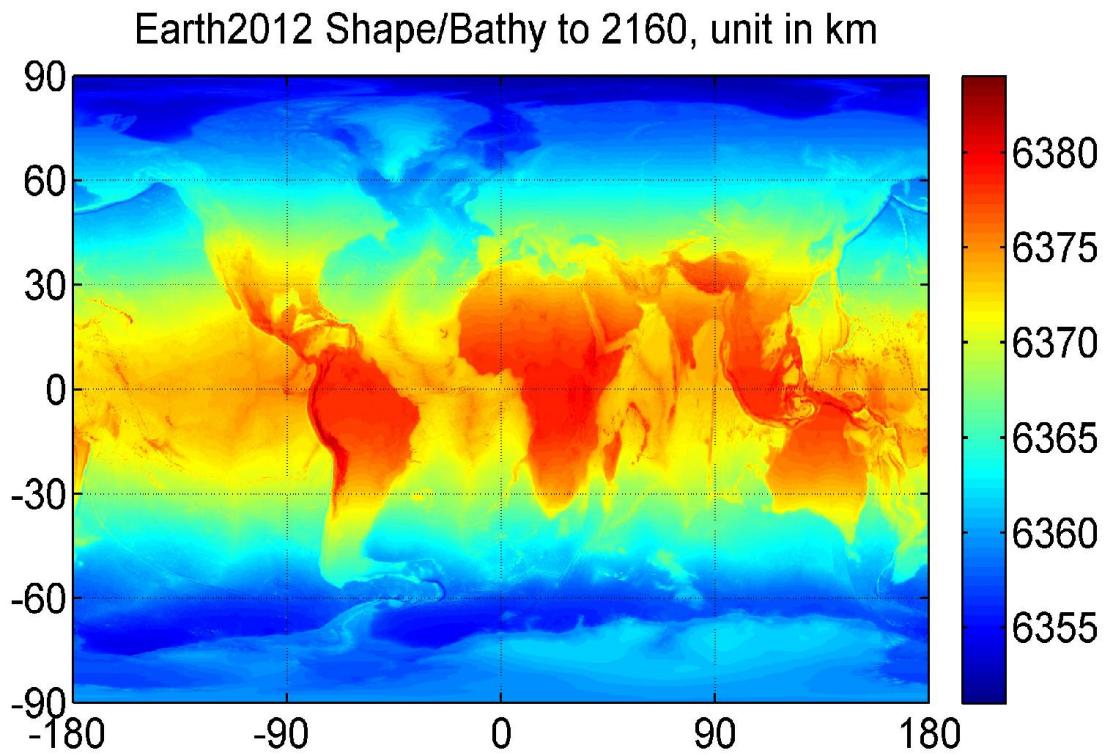




Figure 8 Geocentric distances to Earth Surface.

		ESA Contract:	1/6287/11/I-NB
		Doc. No:	D2100 Preliminary Analysis Report –draft
		Issue: 1	Date: 25.04.14

4. Inland Water



4.1 Satellite altimetry

4.1.1 Introduction

The past 20 years has witnessed increased interest and capability in monitoring inland water using space borne instrumentation. In particular, the availability of satellite altimetry from ERS-2 and ENVISAT and from Jason-1 and Jason-2 is continually adding to the time series of measurements of inland water levels that started with the launch of ERS-1 in 1991 and TOPEX/Poseidon in 1992.

Early results obtained from satellite altimetry utilized the standard altimetric geophysical data records (GDR) produced primarily for oceanographic purposes but with data available over some inland rivers and lakes. For example, Birkett et al. (2002), Coe and Birkett (2004) and Maheu et al. (2003) used TOPEX/Poseidon altimetry over the Amazon, Lake Chad and Plata basin, respectively. Other authors such as Cauhopé et al. (2006), Frappart et al. (2006a), Frappart et al. (2006b) and Leon et al. (2006) utilized TOPEX/Poseidon and ERS/ENVISAT altimetry. These studies either made use of the GDR or estimated heights from the altimetric waveforms using conventional retracker schemes such as the ice-mode tracker (Ice-1) of ENVISAT.

The reliance on standard products or derivations using retrackerers for ice/ocean surfaces places limitations on the geographical coverage to large lakes and rivers. For radar altimeters, the echoes are strongly affected by topography which may cause the altimeter to lose lock resulting in data outages. Alternatively, the altimeter may return an echo from a water surface off-nadir giving rise to large errors in the range. The complexity of the reflecting surface will result in waveform echoes that differ from the single peak of an oceanographic return. Meaningful

		ESA Contract:	1/6287/11/I-NB
		Doc. No:	D2100 Preliminary Analysis Report –draft
		Issue: 1	Date: 25.04.14

results over smaller bodies of waters and in areas of more difficult terrain can be recovered from the multi-peaked returns by utilizing a series of retracking schemes applied to the altimetric waveforms even when the standard retrackers fail to yield results (Berry et al., 2005).

The altimetric water level measurements can be considered as a space borne virtual gauge providing discrete measurements at the repeat cycle of the satellite groundtrack (10-day TOPEX/Poseidon and Jason; 35-day ERS-2 and ENVISAT).



The main constraints for the use of radar altimetry data in hydrology are:

- Temporal resolution
- Spatial resolution
- Accuracy of the level measurement

In the future, if sufficiently high spatio-temporal resolution and accuracy can be achieved; secondary characteristics such as spatial and temporal derivatives of water level can be extracted from the radar altimetry dataset, which are of major interest in hydrology. Moreover, the high along-track resolution of the SAR altimeter onboard Sentinel-3 may enable the measurement of high-resolution water level transects across rivers and river-floodplain systems. Such dataset will provide new insights into the hydrological processes and phenomena occurring in such systems.

4.1.2 Rivers and Lakes project

The Rivers and Lake project (<http://tethys.eaprs.cse.dmu.ac.uk/RiverLake/shared/main>) used satellite altimetry over inland water to provide historical and Near-Real Time (NRT) data for a large number of virtual stations around the world. These are shown in Figure 9. The data is from ENVISAT for the period 2002-2010 and Jason-2 for the period 2009 – present.

		ESA Contract:	1/6287/11/I-NB
		Doc. No:	D2100 Preliminary Analysis Report –draft
		Issue: 1	Date: 25.04.14

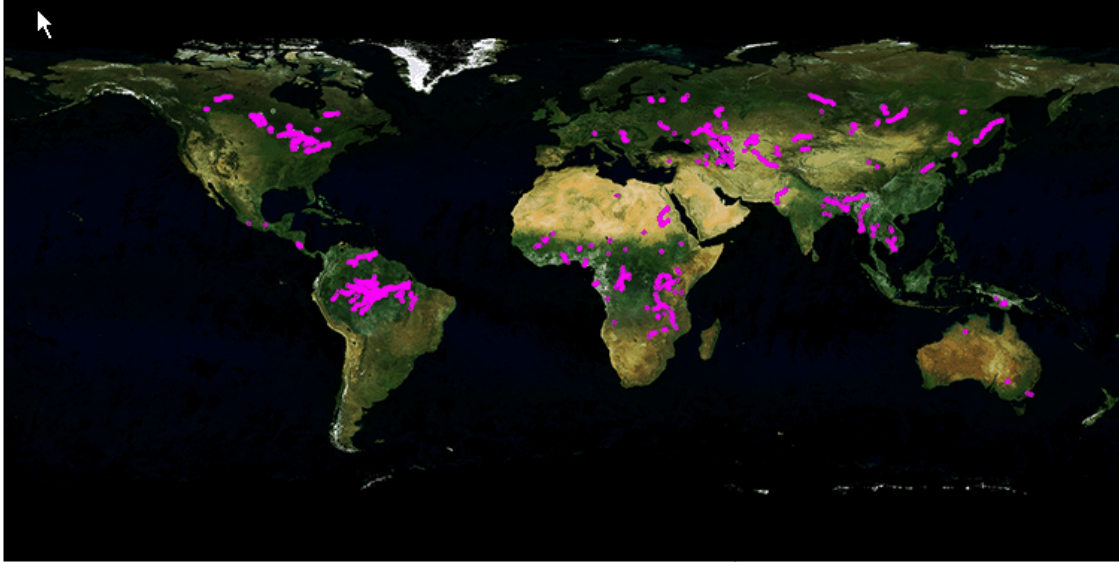






Figure 9 River and Lake global locations

The data for these was derived using the retracking methodology detailed in Berry et al. (2005) based on the 20 Hz ERS-2 and 18 Hz ENVISAT altimetric waveforms. Land is a relatively poor reflector of Ku-band energy compared with inland water so the response from the water target frequently dominates the altimeter return. Complex echo shapes are still returned from land/water composite surfaces and where components other than the inland water response are significant. Each waveform is independently analysed; echoes containing complex shapes (generally resulting from a combination of land and water response or the presence of bright off-nadir reflectors contaminating the nadir response) have been filtered out prior to height determination and a suite of retrackers configured for the different waveform shapes are used to retrack each waveform to obtain the best range to surface estimate. Altimeter heights that pass the quality checks are combined to provide a single stage measurement for the river crossing. The along track displacement between consecutive waveforms is approximately 350 m and the retracker generally provided a single height although multiple heights per crossing were

		ESA Contract:	1/6287/11/I-NB
		Doc. No:	D2100 Preliminary Analysis Report –draft
		Issue: 1	Date: 25.04.14

recovered on occasions. For two heights, a simple average was taken with a two-sigma filter and then averaging utilized for three or more measurements. ENVISAT RA-2 was operated in high precision (ocean) mode over the majority of these targets, changing mode dynamically in response to assessment of its effectiveness in capturing the returned echoes.

In order to assess the accuracy of the satellite altimetry data it is compared against measured in-situ water level data. For example, Figure 10 shows the satellite altimetry crossings and the near-by measured in-situ data for the Mekong river.

		ESA Contract:	1/6287/11/I-NB
		Doc. No:	D2100 Preliminary Analysis Report –draft
		Issue: 1	Date: 25.04.14

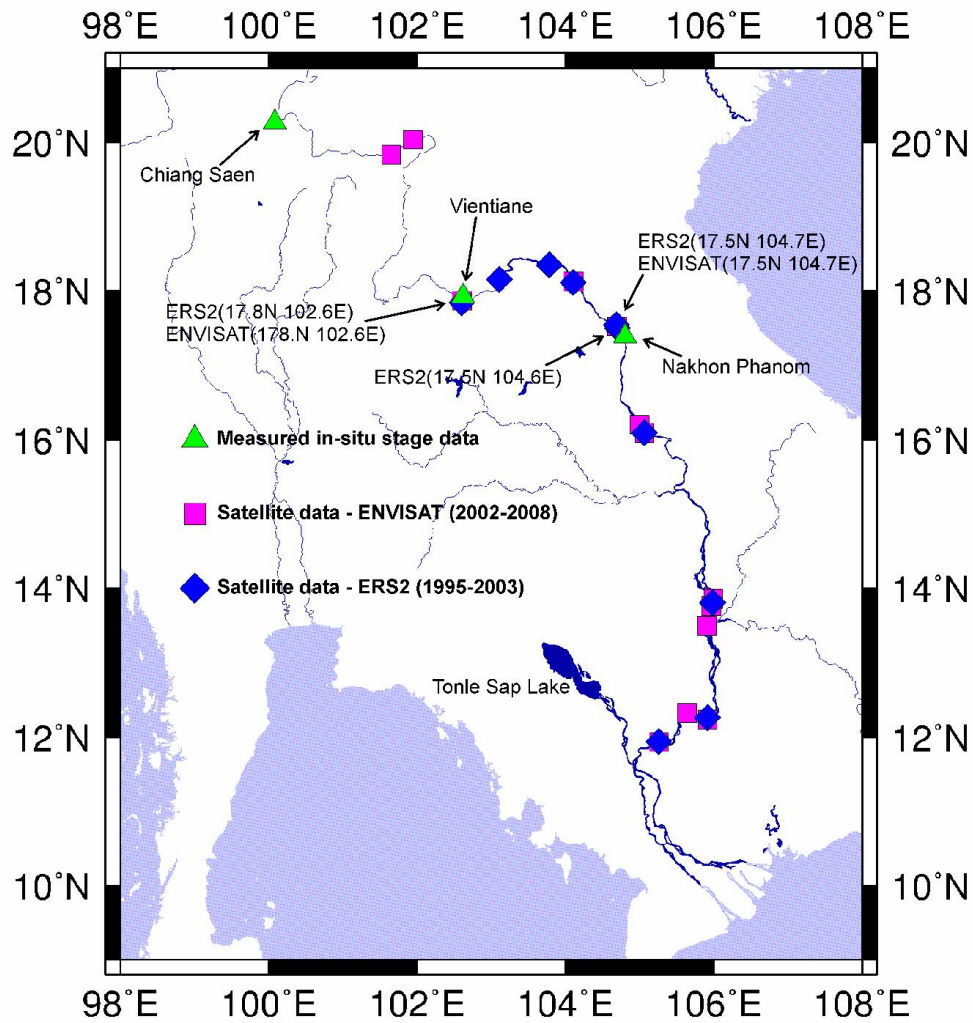




Figure 10 Satellite altimetry crossings and the near-by measured in-situ data for the Mekong river

		ESA Contract:	1/6287/11/I-NB
		Doc. No:	D2100 Preliminary Analysis Report –draft
		Issue: 1	Date: 25.04.14

When compared to measured in-situ data the RMSE errors seem to depend on the channel size, with larger channels having smaller errors. For example Frappart et al. (2006a) found a RMSE of 0.15m for ENVISAT on the Amazon, Birkinshaw et al. (2010) found errors from 0.44m to 0.76m for ERS-2 and ENVISAT on the Mekong and Tarpanelli et al. (2013) found errors from 0.4 – 0.92 for ERS-2 and ENVISAT for the Po river in Italy. Michailovsky et al. (2012) report RMSE between 0.34 m and 1.07 m for 20 ENVISAT virtual stations in the Zambezi River system. In all cases ENVISAT errors were found to be lower than ERS-2 errors.



The bias in satellite altimetry water levels in the Amazon basin is considered by Calmat et al. (2013) using an extensive dataset of gauge zeros measured by GPS at the river gauges. They found a bias of 1.044 +/- 0.212m for the ENVISAT ICE-1 retracked altimetry.

4.1.3 Improvements suggested from Deliverable 1100

In Deliverable 1100 there was a user consultation in which Users suggested improvements that could be made to the Rivers and Lakes data. The main two suggestions were

- More Targets. Figure 9 shows that throughout the world there are a limited number of River and Lake targets. These are targets that have passed the statistical quality control.
- Improved data quality control. Even within those sites that are available (that have passed the quality control) there are a considerable number of outliers or erroneous values. For example, the water level in a lake in some case can be well below the bed level of the lake.

Obviously these two suggestions are related in that many of the targets are not incorporated because they have poor quality.

		ESA Contract:	1/6287/11/I-NB
		Doc. No:	D2100 Preliminary Analysis Report –draft
		Issue: 1	Date: 25.04.14



Following the User consultation it is suggested that in future two sets of data are made available. The first dataset would be a NRT dataset similar to that already available. The second datasets would be a properly validated historical dataset so that full use can be made of this exciting and unique dataset. This would require a reanalysis of all existing data. Three possibilities are suggested for the validation

- A simple range test. For each site there is a maximum possible and minimum possible value. If the data is outside this range it can be removed
- A test for jumps in the data. It can be physically impossible for river water levels to drop more than a certain amount within a 35 day period
- Analysis of nearby data. Birkinshaw et al. (2010) removed erroneous data by considering all the satellite altimetry along a stretch of river simultaneously.



4.2 Repeat orbits and drifting orbits: implications for hydrological applications

For hydrological applications, the orbit configuration is probably the most important difference between Cryosat-2 and earlier satellite radar altimetry missions (ERS-2, ENVISAT etc). The earlier missions were on repeat orbits, i.e. the ground track of the satellite revisited approximately the same locations every 35 days for ENVISAT and ERS-2. In contrast, Cryosat-2 is on a drifting orbit. The exact repeat period is 369 days. The orbit is configured in 30-day sub-cycles. Ground tracks of Cryosat-2 can be downloaded in Google Earth format from <ftp://calval-pds.cryosat.esa.int>.

The difference between repeat and drifting orbits for hydrological applications can be illustrated for the example of the Brahmaputra River. Figure 11 shows the crossing points between the

		ESA Contract:	1/6287/11/I-NB
		Doc. No:	D2100 Preliminary Analysis Report –draft
		Issue: 1	Date: 25.04.14

ENVISAT and ERS-2 repeat orbits and the Brahmaputra River (Michailovsky et al, 2013). For each of these crossing points, water level estimates are available every 35 days. These estimates can be collected to form a virtual station time series, one for each crossing point. The dynamics of the water level at the virtual station locations can be evaluated, compared to in-situ information, transformed into river discharge estimates or assimilated into hydrological models as has been done in many previous studies (Birkinshaw et al. 2010; Michailovsky et al., 2013). This can be done even if the in-situ gauging station data or the hydrological model only provide relative water level, i.e. water level that is not referenced to mean sea level. No common height reference between the water level estimates from radar altimetry and the in-situ measurements or model estimates is required because any bias can be removed by matching the mean of the two time series. Moreover, consistency of the time series can be checked and obvious outliers are easily detected. Most if not all previous studies exploiting radar altimetry for hydrological applications have used virtual station time series.

		ESA Contract:	1/6287/11/I-NB
		Doc. No:	D2100 Preliminary Analysis Report –draft
		Issue: 1	Date: 25.04.14

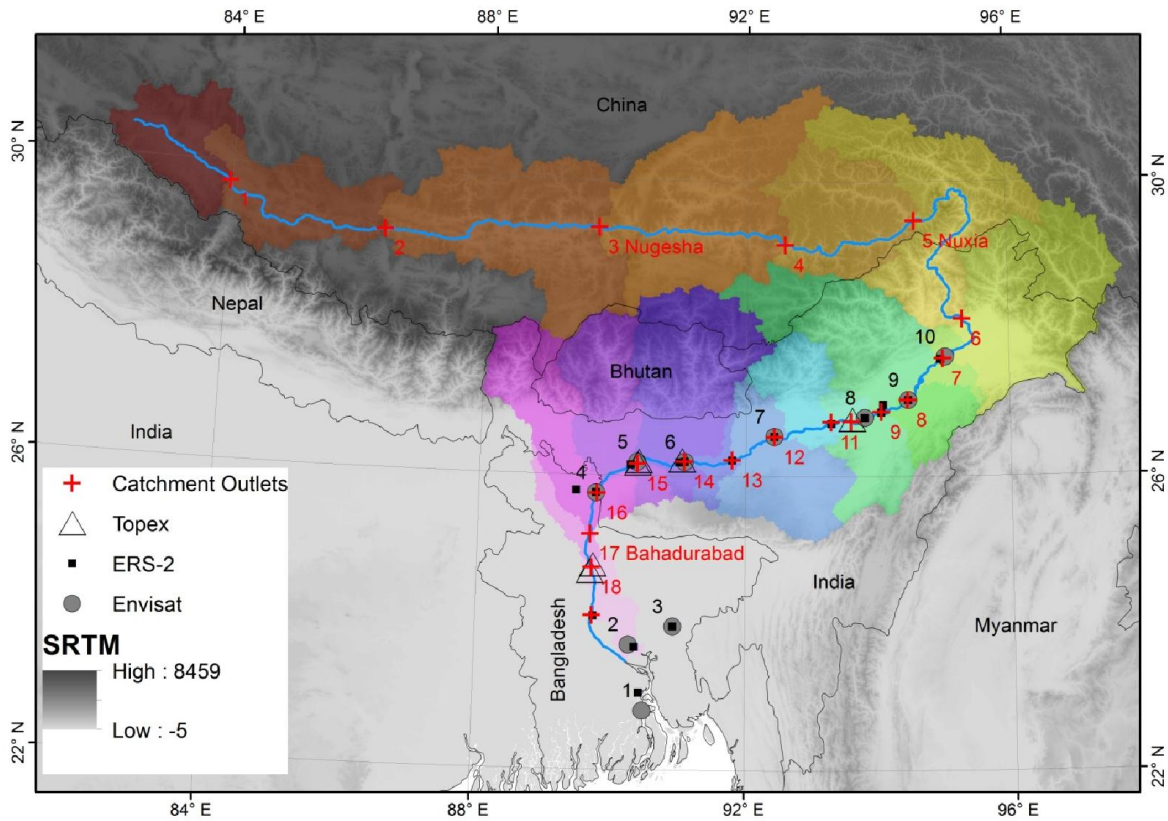


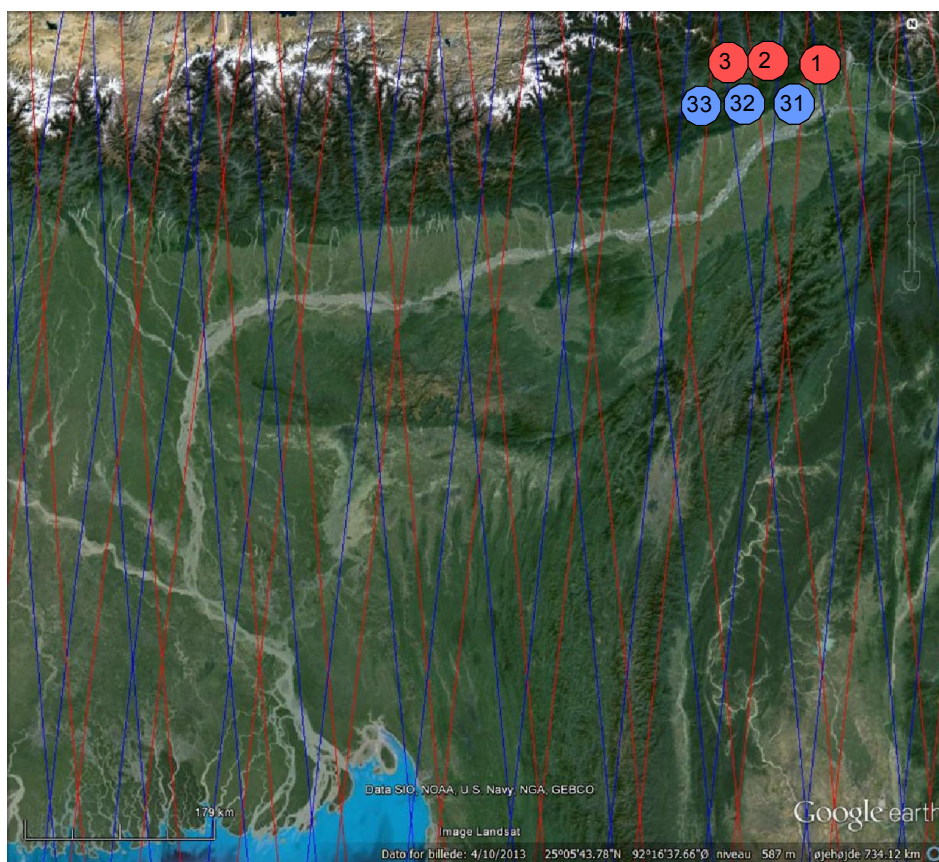


Figure 11 ENVISAT and ERS-2 virtual stations on the Brahmaputra River

Figure 12 shows the Cryosat-2 orbit configuration over the Brahmaputra for two selected consecutive sub-cycles (indicated as red and blue lines). During the red sub-cycle, the river is sampled at daily intervals for about 15 days with measurement locations cascading downstream in steps of a few tens of kilometers. During this period, there is a measurement somewhere on the river every day, but every day in a different location. After approximately 15 days, the orbits do no longer cross the Brahmaputra River and no data on this river will be collected for the remainder of the sub-cycle, i.e. about 15 days. The same happens for the second sub-cycle, i.e. again there will be a 15-day period with daily data followed by a 15-day period without any data.

		ESA Contract:	1/6287/11/I-NB
		Doc. No:	D2100 Preliminary Analysis Report –draft
		Issue: 1	Date: 25.04.14



Moreover, sampling locations in sub-cycle 2 will be shifted relative to sub-cycle 1. It takes 369 days, i.e. more than one year, before the exact same locations are sampled again.



Two Sub-cycles
 Relative overpass time in days

Figure 12 Cryosat-2 orbits over the Brahmaputra River. Red orbits belong to a first sub-cycle and blue orbits to a second sub-cycle. Numbers indicate relative overpass times in days.

The unconventional Cryosat-2 sampling pattern has implications for quality control of the derived water level estimates. Time series consistency can no longer be used, instead spatial

		ESA Contract:	1/6287/11/I-NB
		Doc. No:	D2100 Preliminary Analysis Report –draft
		Issue: 1	Date: 25.04.14



consistency along the river could be used. However, it is important to remember that the river water table is a dynamic surface and the slope of the river water table will change in time.

The unconventional Cryosat-2 sampling pattern also has important implications for the assimilation of the data to river models. Because the mission provides data basically from any point on the river, models are required that simulate the river water table at any point along the river. This calls for a 1-dimensional or 2-dimensional full hydrodynamic river model solving the Saint-Venant equations for shallow water flow (e.g. Chow et al, 1988). Many software packages exist that implement this solution (e.g. Mike-11, HEC-RAS etc.). However, such models require cross-sectional geometry of the river as a model input. Cross-sectional geometry is a key factor for water level dynamics because it controls the balance between friction forces and gravity. If the river is confined to a narrow cross section water level change per unit change in river discharge will be larger than in a wide cross section. Hydrodynamic models are generally non-linear. Ensemble approximations of the Kalman Filter provide suitable data assimilation strategies to combine models and radar altimetry data.

It is clear that using Cryosat-2 data to inform river models requires different modeling and assimilation approaches from those used for virtual station data. Most likely, the requirement for in-situ cross section information will be the bottleneck for the application of such modeling and assimilation technology, particularly in large and remote river basins. Because it is hard to check consistency of the water level estimates due to the long orbit repeat, it is important that realistic error estimates be reported along with the water level estimates from radar altimetry.

4.3 Rivers

Knowledge of the variability in river discharge is of fundamental importance to planners managing flood hazards and water resources and to scientists concerned with climate change.

		ESA Contract:	1/6287/11/I-NB
		Doc. No:	D2100 Preliminary Analysis Report –draft
		Issue: 1	Date: 25.04.14



However, assessment of river discharge is severely constrained by lack of measurements of flows at the catchment scale (Vörösmarty et al., 2010). Over much of the Earth availability of in situ gauge data of stage (or level) and discharge has declined over the past decades. For example, there has been a 66% reduction in operational gauges since 1985 (Nijssen et al., 2001) in northern latitudes while stations in the R-Arctic net dataset declined from 1198 operating between 1960 and 1985 to just 280 operating between 1985 and 2000.

Satellite altimetry has the potential to overcome the problems with the lack of data. However, the main problem is converting the water level (stage) to the discharge. Bjerklie *et al.* (2003), Alsdorf *et al.* (2007) and Tang *et al.* (2009) have reviewed the various satellite data sources and their potential, detailing a number of different techniques that make use of remote sensing to estimate river discharge.

4.3.1 In-situ measured discharge data

The best source of global scale measured in-situ data is the Global Runoff Database Collection (GRDC) database (http://www.bafg.de/GRDC/EN/Home/homepage_node.html). GRDC is a unique collection of river discharge data collected at daily or monthly intervals from nearly 9000 stations in 157 countries. This adds up to around 360.000 station-years with an average record length of 40 years. The GRDC provides discharge data and data products for non-commercial applications. Other potential sources of international measured in-situ data (mostly monthly) include:

- The Global River and Delta Systems dataset information page (http://csdms.colorado.edu/wiki/Data:Global_River_and_Delta_Systems)



		ESA Contract:	1/6287/11/I-NB
		Doc. No:	D2100 Preliminary Analysis Report –draft
		Issue: 1	Date: 25.04.14

- R-ArcticNet (v4.0) - A Regional, Electronic, Hydrographic Data Network For the Arctic Region (<http://csdms.colorado.edu/wiki/Data:R-ArcticNet>)
- SAGE - a compilation of monthly mean river discharge data for over 3500 sites worldwide. (<http://csdms.colorado.edu/wiki/Data:Sage>)

4.3.2 Stage-discharge relationship

The standard method to obtain a continuous measurement of river discharge is to monitor river water level data and convert it to discharge using a stage-discharge relationship. Water level data is typically recorded with pressure transducers or automatic water level recorders. In developed countries, such stations are installed and maintained at regular intervals (typically 10s of kilometers) along all significant rivers. Data are transferred in real-time via the mobile network and are archived and processed by relevant agencies. Many countries provide free and web-based access to such datasets, while in other countries, this information is classified and hard to obtain. Typically, the accuracy of the equipment is better than one centimeter and the temporal resolution is a few minutes or less. In developing countries, the density and quality of the in-situ station network is much worse and there are many indications that the in-situ monitoring capability for surface waters has been declining at the global scale over the past two decades (Fekete and Vorosmarty, 2007).

To calculate the stage-discharge relationship measurements of river discharge are needed over a range of water levels. Direct measurements of river discharge data are obtained from cross-sectional measurements of water velocity or from Acoustic Doppler Current Profiling (ADCP), see Figure 13. ADCP uses Doppler reflection of ultrasound waves on suspended particles in the river current to obtain current velocity, and bottom reflections to obtain depth. River discharge

		ESA Contract:	1/6287/11/I-NB
		Doc. No:	D2100 Preliminary Analysis Report –draft
		Issue: 1	Date: 25.04.14

is obtained as the integral of current velocity over the entire river cross section. ADCP is an efficient technology and the accuracy is around 10% (Muste et al., 2004). ADCP field work does not require a tagline, as the exact transect of the boat can be taken into account when processing the data. The river cross section method (Figure 14) is more tedious and time consuming. First, a tagline has to be installed across the river. Then, water velocity is measured at regular intervals and depths across the river, using propeller current meters. Again, total discharge is computed as the integral of current velocity over the entire section. At permanent discharge stations, the tagline is typically a permanent installation, and current profiling is done automatically from a control station on the shore.

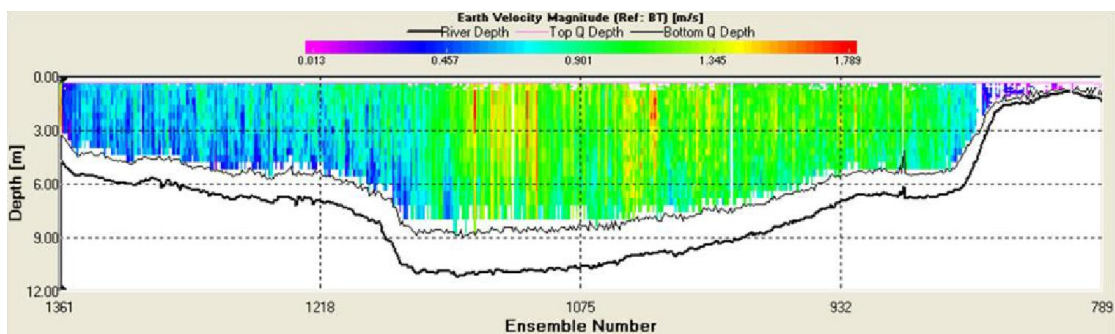




Figure 13 ADCP cross section of the Zambezi River

		ESA Contract:	1/6287/11/I-NB
		Doc. No:	D2100 Preliminary Analysis Report –draft
		Issue: 1	Date: 25.04.14

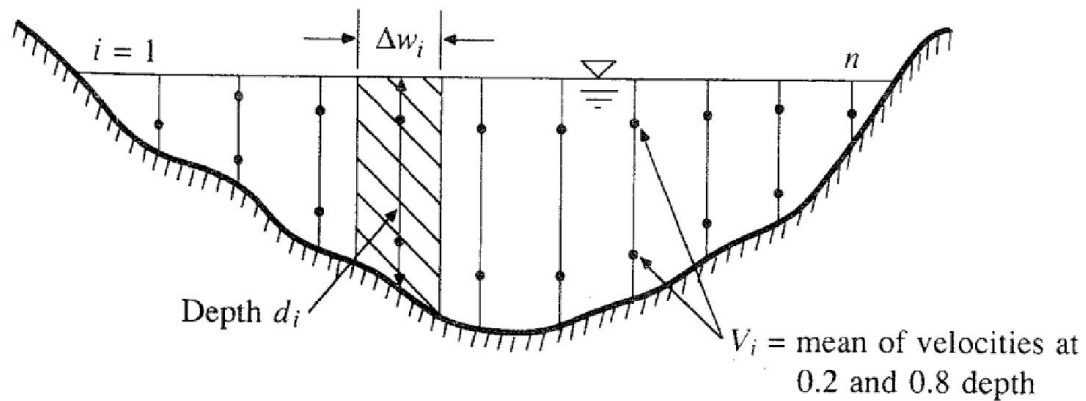




Figure 14 Cross-section method to measure river discharge (from Chow et al., 1988).

The stage-discharge relationship (or rating curve) is a relationship between water level and discharge based on a number of co-incident measurements of water level and discharge (Figure 15). Typically a polynomial relationship or power-law is fitted through the data points and is used to estimate discharge from level. A major issue is the stability of rating curves over time. In natural rivers, bank erosion and sediment transport will change the rating curve and the relationship should therefore be updated at regular intervals. Table 1 summarizes the main characteristics of traditional and radar altimetry data for hydrological applications

		ESA Contract:	1/6287/11/I-NB
		Doc. No:	D2100 Preliminary Analysis Report –draft
		Issue: 1	Date: 25.04.14

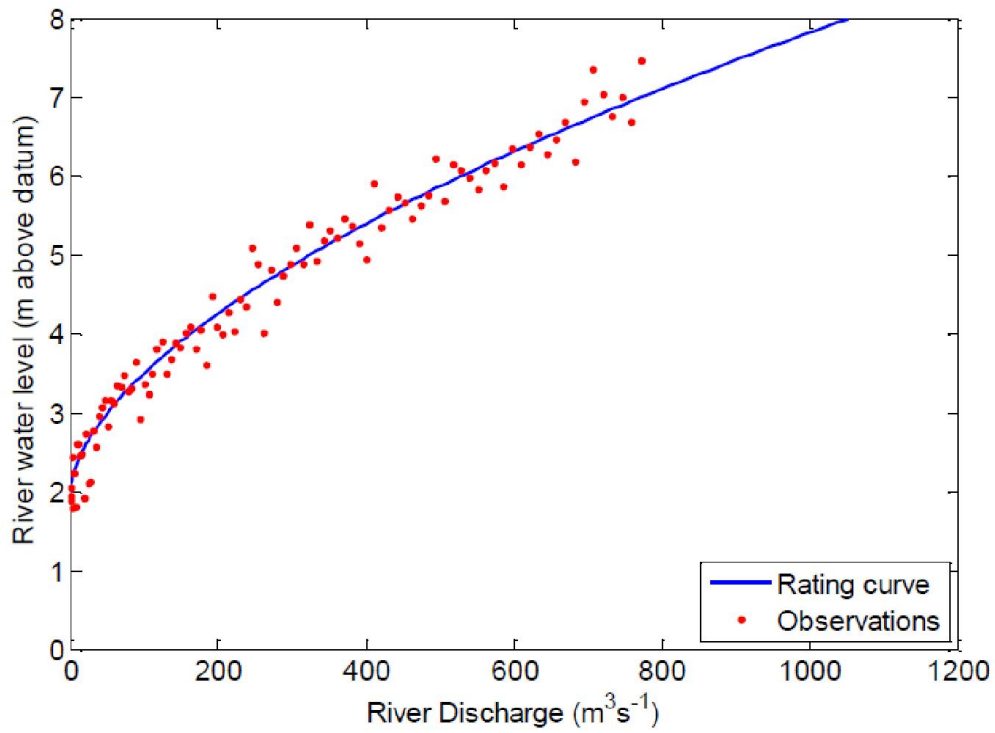


Figure 15 Example of a rating curve describing the relationship between water level and discharge





		ESA Contract:	1/6287/11/I-NB
		Doc. No:	D2100 Preliminary Analysis Report –draft
		Issue: 1	Date: 25.04.14

Table 1 Main characteristics of in-situ datasets and hydrological datasets derived from radar altimetry.

	In-situ water level	In-situ discharge	Water level from radar altimetry
Temporal resolution	From seconds to days	From seconds to days	Tens of days
Spatial resolution	Tens of kilometers	Tens of kilometers	Tens to hundreds of km for virtual stations, hundreds of m for transects
Accuracy	Sub-cm	10%	Around 0.5 m
Coverage	Dense in some regions, zero elsewhere	Dense in some regions, zero elsewhere	Distributed evenly over areas of the same latitude. Increasing density towards the poles.

4.3.3 Hydrological modeling

Figure 16 shows a map of the major river basins of the world. For most of these river basins, hydrological models have been developed. Modeling approaches and implementations vary widely and range from conceptual lumped-parameter models to fully distributed, physically-based models. (Nijssen et al., 2001) simulated 26 of the major rivers basins using the VIC macroscale hydrological model with a 2° by 2° model grid cell for land surface characteristics such as elevation, soil, and vegetation. River routing was carried out on a 1° by 1° grid. The selected basins included the Amazon, Congo, Mississippi, Ob, Lena, Yenise, Yellow and Yangtze. Werth et al. (2009) and Werth and Guntner (2010) used the WaterGAP Global Hydrology Model (WGHM) for 28 of the largest river basins worldwide. Five years (January 2003-December 2007) of satellite-based estimates of the total water storage changes from the GRACE mission were combined with river discharge data in a multi-objective calibration framework that uses the most sensitive WGHM model parameters. Other models include those by (Ward et al., 2007;

		ESA Contract:	1/6287/11/I-NB
		Doc. No:	D2100 Preliminary Analysis Report –draft
		Issue: 1	Date: 25.04.14



Qian et al., 2006; Coe, 2000). If no in-situ measurements of water levels are available, satellite altimetry can be a valuable data source, which, when assimilated to some of the above models, can confine hydrological predictions.

4.3.4 River Uses 1 - Large and Poorly gauged river basins

Many of the planets major river basins (e.g. in the Arctic, in Africa) are poorly gauged or ungauged. In such river basins, radar altimetry represents a significant monitoring capability (the user requirements are shown in Table 2). The main problem in using satellite altimetry for these locations is obtaining the river discharge from the altimetry water levels. Various methods have been tested and developed depending on the available data, the type of river and the local requirements

The satellite altimetry can be used together with hydrological models (see 4.3.3) to provide river discharges (Andreadis *et al.*, 2007; Getirana, 2010; Milzow *et al.*, 2011; Pereira-Cardenal *et al.*, 2011). Recent studies by Michailovsky et al. (2013) and Michailovsky and Bauer-Gottwein (2014) have explored the potential of radar altimetry for real-time operational river-basin modelling and have assimilated nadir altimetry data over the Brahmaputra and Zambezi rivers into Muskingum-type river routing schemes. Alternatively, rating curves can be created by combining the satellite altimetry data and *in situ* measured discharge data (Kouraev *et al.*, 2004; Zakharova *et al.*, 2006; Papa *et al.*, 2010) or with the discharge calculated using the Muskingum–Cunge approach (Leon *et al.*, 2006).

Bjerklie et al. (2003) considered the potential of estimating river discharge entirely from remotely sensed data sources. The authors suggest that models based on width, depth and slope have generally greater accuracy, especially for large rivers, compared to alternative models that include only width and slope or width, slope and velocity. In a follow-on paper Bjerklie et al. (2005) used SAR and slope data to estimate discharge and suggest that the

		ESA Contract:	1/6287/11/I-NB
		Doc. No:	D2100 Preliminary Analysis Report –draft
		Issue: 1	Date: 25.04.14



inclusion of altimetry data could improve the estimates. Birkinshaw et al. (2010) used altimetry data together with in situ measured channel cross-sections to estimate discharge at an ungauged site and again emphasized the potential of using remote sensing, such as SAR, to provide information on the channel cross-sections. Barbetta and Moramarco, (2014) used altimetry data at a virtual station together with upstream measured discharge to estimate discharge at the virtual station. Birkinshaw et al. (2014) estimated discharge at an ungauged site using both satellite (ERS-2 and ENVISAT) altimetry data to provide river channel stage data and channel slope, and Landsat satellite imagery to provide a series of channel widths and hence channel cross-sections. Gleason and Smith (2014) use characteristic a scaling law fundamental to natural rivers and Landsat Thematic Mapper images to estimate the discharge using no in-situ measured data.

The assimilation of altimetric water level data into high-resolution hydrodynamic models for flood protection and management has also been carried out. Because this approach requires high spatial resolution, most studies have used synthetic datasets with characteristics similar to what is expected from the Surface Water and Ocean Topography (SWOT) mission (e.g. Andreadis et al., 2007; Biancamaria et al., 2011; Durand et al., 2008).

Table 2 User requirements for the large and poorly-gauged river basins use case.

Minimum requirement for radar altimetry water level product	
Temporal resolution	Tens of days
Spatial resolution	Tens to hundreds of km
Accuracy	0.5 m
Coverage	Large river basin scale

Figure 16 shows in which basins altimetry has been used to date. Due to its size and importance, the Amazon River basin has been the showcase application case study for inland water monitoring using radar altimetry. However, over recent years, several much smaller rivers

		ESA Contract:	1/6287/11/I-NB
		Doc. No:	D2100 Preliminary Analysis Report –draft
		Issue: 1	Date: 25.04.14

have also been monitored successfully (e.g. Zambezi, Mekong). Rivers as narrow as 100 m could be detected and monitored using nadir altimetry from the ENVISAT platform.

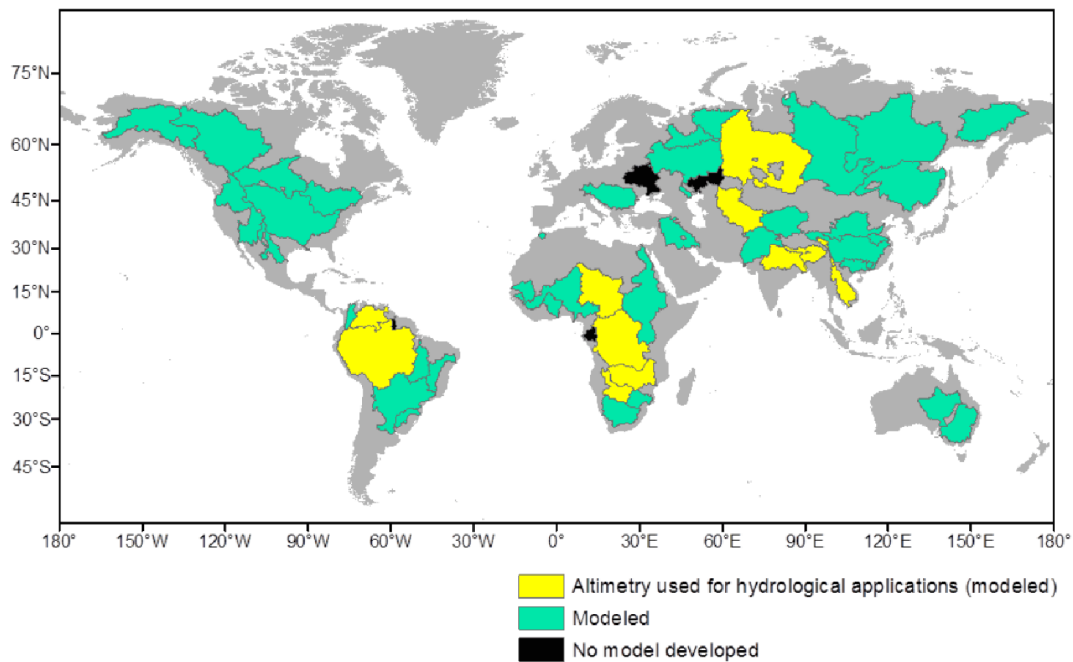




Figure 16 Major river basins of the world. Hydrological model development and use of radar altimetry (adapted from Bauer-Gottwein et al., 2013).

The other main method to obtain river discharges is to use remote sensing data to provide information on the river width. This information is often provided using a passive microwave sensor, AMSR-E. This technique is particularly useful in channels where there is a large change in width as the discharge increases. The Global Flood Detection System (GFDS , <http://www.gdacs.org/flooddetection/>), uses the AMSR – E sensor, together with the Tropical Rainfall Measurement Mission (TRMM) Microwave Imager (TMI), to measure surface brightness temperatures , which can be used to infer streamflow and thus show the potential



		ESA Contract:	1/6287/11/I-NB
		Doc. No:	D2100 Preliminary Analysis Report –draft
		Issue: 1	Date: 25.04.14

to monitor floods over the globe (Brakenridge et al. , 2007) . Other studies have also evaluated the potential application of the AMSR - E sensor for discharge estimation and flood detection (Temimi et al. , 2007; Temimi et al. , 2011; Salvia et al., 2012) , but they all require measured in-situ streamflow information. Brakenridge et al. (2012) and Zhang et al. (2014) use the passive microwave without in-situ streamflow observations, in a hydrologic model. The remote-sensing data are assimilated into the hydrological model in order to demonstrate probabilistic flood prediction for an African basin. The Dartmouth Flood Observatory also uses the NASA AMSR-E satellite microwave data. This is used to detect, measure, and map river discharge and river flooding. It produces a remote sensing signal that tracks river discharge at 2500+ carefully selected river measurement sites. Flooding is monitored by the MODIS sensors, to map floods as they occurred. (<http://floodobservatory.colorado.edu/>)

4.3.5 River Uses 2 - Flood Dynamics and River-floodplain interactions

One of the advantages of new SAR-altimetry technology is the high along-track resolution. Potentially, this can be used to resolve small-scale water level variations in river and wetland systems and may provide new insights in floodplain-channel interactions and water budgets. Findings may have a direct impact on the exploitation of the upcoming SWOT mission. For this use case Doppler beam steering for known locations with open water is preferable. The user requirements for this use case are listed in Table 3.

Previously research on this subject has been carried out in the north of the Western Siberian Plain using the ENVISAT data. In these studies ENVISAT RA-2 radar altimetry data have been used to estimate seasonal wetland extent variability for the Poluy, Nadym, Pur and Taz rivers (Zakharova et al., 2009; Zakharova et al., 2011).

		ESA Contract:	1/6287/11/I-NB
		Doc. No:	D2100 Preliminary Analysis Report –draft
		Issue: 1	Date: 25.04.14

River-groundwater dynamics have been studied by Pfeffer et al. (2014). They used concepts from groundwater-surface water interactions and ENVISAT altimetry data, in order to evaluate the topography of the groundwater table during low-water periods in the alluvial plain of the central Amazon. The water levels were monitored using 491 altimetric stations over surface waters in the central Amazon. The groundwater table maps were interpolated at spatial resolutions ranging from 50 to 100 km are consistent with groundwater wells data.

Table 3 User requirements for river-floodplain interaction use case

Minimum requirement for radar altimetry water level product	
Temporal resolution	Tens of days
Spatial resolution	Hundreds of meters
Accuracy	0.1 m
Coverage	Local scale

4.3.6 River Uses 3: Continental-scale water balance monitoring

One clear advantage of radar altimetry over traditional in-situ monitoring datasets is the global coverage. To fully exploit this advantage, radar altimetry should be used jointly with global inland water simulators to produce consistent estimates of continental-scale water budgets and inland water dynamics. To our knowledge, no global operational hydrological model has been informed with radar altimetry data to date. However, several authors have published preliminary studies and results to support this research direction (Yamazaki et al., 2011; Yamazaki et al., 2012). For this use case, time series at virtual stations are the preferred data delivery format.



		ESA Contract:	1/6287/11/I-NB
		Doc. No:	D2100 Preliminary Analysis Report –draft
		Issue: 1	Date: 25.04.14

Table 4 User requirements for continental-scale water balance monitoring use.



Minimum requirement for radar altimetry water level product	
Temporal resolution	Tens of days
Spatial resolution	Tens to hundreds of km
Accuracy	0.5 m
Coverage	Continental scale/global

4.4 Lakes

The altimetry water levels in lakes can be used directly to provide useful information for a variety of water balance and long-term trend studies. Most of the large natural lakes have measured in-situ water level data which is available for these studies. But for many of the reservoirs and small water bodies this in-situ data is not available.



4.4.1 In-situ and satellite altimetry Water Level data

Individual in-situ data is available for many individual lakes. The best international database is currently the International Data Centre on Hydrology of Lakes and Reservoirs - HYDROLARE (<http://www.hydrolare.net/>). HYDROLARE was established in 2009 in St Petersburg, Russia by ROSHYDROMET at the State Hydrological Institute. HYDROLARE provides data on nearly 550 world lakes and reservoirs. It operates under the auspices of the world Meteorological Organization (WMO).

		ESA Contract:	1/6287/11/I-NB
		Doc. No:	D2100 Preliminary Analysis Report –draft
		Issue: 1	Date: 25.04.14

The Rivers and Lakes project (<http://tethys.eaprs.cse.dmu.ac.uk/RiverLake/shared/main>) provides satellite altimetry data over a number of lakes throughout world (Figure 9). Another good source of data for satellite altimetry lake levels is the LEGOS HYDROWEB site (<http://www.legos.obs-mip.fr/soa/hydrologie/hydroweb/>). The database (Crétaux et al. 2011) contains time series over water levels of large rivers, lakes and wetlands around the world. These time series are mainly based on altimetry data from Topex/Poseidon for rivers, but ERS-1 & 2, ENVISAT, Jason-1 and GFO data are also used for lakes. At present, water level time series of about 100 lakes (in Europe, Asia, Africa, North and South America) including the Aral and Caspian seas are available. About 250 sites (called virtual stations) on large rivers are also available (see Figure 17). The United States department for Agriculture (USDA, 2011) also provides lakes levels using satellite altimetry data. Their database contains water levels from 78 sites using Jason-2 data and 148 sites from ENVISAT data (http://www.pecad.fas.usda.gov/cropexplorer/global_reservoir/). Figure 18 shows details of which lakes and reservoirs are in the database.

The accuracy of ENVISAT radar altimetry water levels over Lake Issykkul in Kyrgyzstan have been considered in detail in Cretaux et al. (2013). This was chosen as a calibration/validation site in 2004 and the sources of errors are discussed in detail in this work.

		ESA Contract:	1/6287/11/I-NB
		Doc. No:	D2100 Preliminary Analysis Report –draft
		Issue: 1	Date: 25.04.14

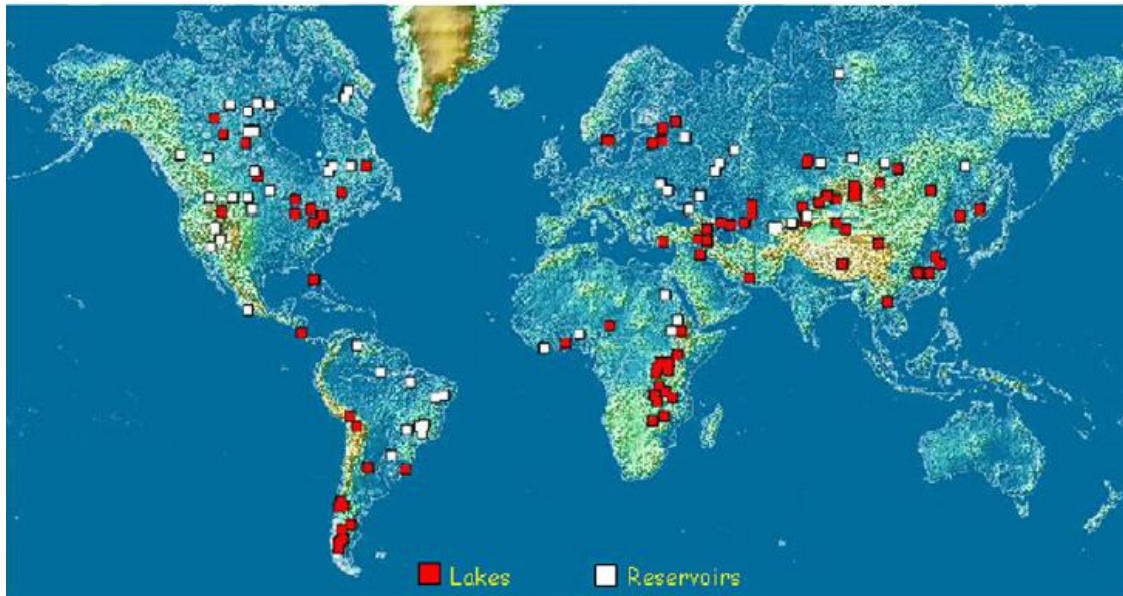


Figure 17 Map of the existing lakes and reservoirs of the HYDROWEB database





		ESA Contract:	1/6287/11/I-NB
		Doc. No:	D2100 Preliminary Analysis Report –draft
		Issue: 1	Date: 25.04.14



Figure 18 Map of the existing lakes and reservoirs of the USDA database

		ESA Contract:	1/6287/11/I-NB
		Doc. No:	D2100 Preliminary Analysis Report –draft
		Issue: 1	Date: 25.04.14

4.4.2 Lakes Uses 2: Long-term water level trends

Radar altimetry from ERS and ENVISAT has been collected consistently for the past almost 20 years at the global scale (GAO Et Al., 2012; Ricko et al., 2012). The availability of consistent long-term records provides an opportunity to quantify effects of global change on the global water budget. Continental freshwater storage in lakes and reservoirs may become a similarly important climate change indicator as for instance global sea level rise and ice mass loss. There are several recent examples of the use of altimetry levels in lakes for this sort of analysis. Duan and Bastiaanssen (2013) estimated water volume variations in lakes and reservoirs from four operational satellite altimetry databases and satellite imagery data. Moore and Williams (2014) used water level data from ENVISAT together with GRACE data and the GLDAS model to look at trends in groundwater change in Africa from 2003-2011. Longuevergne et al. (2013) also use GRACE and altimetry data in lakes looking at trends in the Middle East. Van Dijk et al. (2013) use GRACE, altimetry data in lakes and a hydrological model analyzing global water cycle between 2003 and 2012.

A combination of simultaneous active and passive data from radar altimeters and passive microwave observations from SMMR-SSM/I has also been successfully used for studies of freezing and melting processes of the five largest Eurasian continental water bodies – the Caspian and Aral seas, and the Baikal, Ladoga and Onega lakes (Kouraev et al., 2008; Kouraev et al., 2009). The user requirements for this use case are listed in Table 5.



		ESA Contract:	1/6287/11/I-NB
		Doc. No:	D2100 Preliminary Analysis Report –draft
		Issue: 1	Date: 25.04.14

Table 5 User requirements for the long-term water level trends use case

Minimum requirement for radar altimetry water level product	
Temporal resolution	Tens of days
Spatial resolution	Tens to hundreds of km
Accuracy	0.1 m
Coverage	Global
Temporal consistency	Decades

4.4.3 Lakes Uses 2: Large ensembles of small water bodies

Some hydrological systems on the planet are characterized by large numbers of small water bodies, which, due to their large number and remote location, are difficult to monitor in-situ. Examples include ephemeral water bodies in the Sahel, lake ensembles in the Arctic and ensembles of sinkholes, e.g. in the Yucatán karst aquifer, Mexico. Radar altimetry offers a unique monitoring capability for such systems (Smith and Pavelsky, 2009). Zakharova et al. (2014) uses altimetric data from ENVISAT to analyze seasonal variability of wet zones and water levels in the northern part of Western Siberia which is characterized by a large number of lakes, fens, string bogs etc. Whereas, Baup et al. (2013) show the potential of using satellite altimetry data and high-resolution (HR) images to determine the volume of water in small lakes (<100 ha). Santos da Silva et al. (2012) used satellite altimetry for a section of the Amazon containing rivers, floodplains, wetlands and lakes. Khajeh, et al. (2013) used satellite altimetry for a wetland in Louisiana.

For this use case, heights as a function of space and time are the preferred delivery format. Doppler beam steering for known locations with open water also has potential.





		ESA Contract:	1/6287/11/I-NB
		Doc. No:	D2100 Preliminary Analysis Report –draft
		Issue: 1	Date: 25.04.14

Table 6 User requirements for the large ensembles of small water bodies use

Minimum requirement for radar altimetry water level product	
Temporal resolution	Tens of days
Spatial resolution	Tens of km
Accuracy	0.5 m
Coverage	Regional/catchment scale

		ESA Contract:	1/6287/11/I-NB
		Doc. No:	D2100 Preliminary Analysis Report –draft
		Issue: 1	Date: 25.04.14

5. Conclusions and Recommendations



ESA's Cryosat-2 mission is the first one carrying a radar altimeter that can operate in SAR mode. Its primary aim is land and marine ice monitoring but the high along-track sampling of Cryosat-2 altimeter in SAR mode thus offers the opportunity to recover high frequency signals over much of the Earth's land surface, contributing to mapping applications, and transforming the inland water height retrieval capability.

This deliverable started with some preliminary analysis, common to both land and inland water applications, of the waveforms from Cryosat-2 LRM, SAR and SARIN data.

Considering the land and water theme the review then considered the following:



- Detailed analysis of accessible data sets (space and in-situ) that can be used for development and validation.
- Models that are available including data integration approaches as well as their related limitations, drawbacks and challenges.
- Thorough review of the most current scientific publications

From the review of the Global Digital Elevation Models it is clear this data is used by a vast number of people in a large number of different fields. Most research makes use of the existing SRTM and ASTER data, which is extremely well used, but contains considerable errors in vertical accuracy. There are also problems where there are high mountains, deserts, lakes and forests. The ACE2 dataset, which uses satellite altimetry together with the SRTM, has the potential to overcome these problems but it is currently under-utilized.

		ESA Contract:	1/6287/11/I-NB
		Doc. No:	D2100 Preliminary Analysis Report –draft
		Issue: 1	Date: 25.04.14

The review shows that there is a considerable amount of research being carried out on lakes and rivers. There is some measured in-situ data available (GRDC and HYDROLARE) but this data is being augmented by satellite altimetry data for both lakes and river (e.g. the Rivers and Lakes (<http://tethys.eaprs.cse.dmu.ac.uk/RiverLake/shared/main> and HYDROWEB at LEGOS (<http://www.legos.obs-mip.fr/soa/hydrologie/hydroweb/>)). There are limitations in the current satellite altimetry data both in its quality (errors and in particular erroneous data) and its limited availability (the restricted number of virtual stations). Cryosat-2 and in future Sentinel-3 have massive potential to improve the quality and range of this data and so its potential use in vast range of research projects.

This Deliverable 2100 (D2100) was part of work Package 2000 (WP 2000). The other deliverable in WP 2000 is the Development and Validation plan – Deliverable 2200 (D2200). In D2200 a detailed plan for the tasks and test sites that will be carried in this research contract will be outlined

		ESA Contract:	1/6287/11/I-NB
		Doc. No:	D2100 Preliminary Analysis Report –draft
		Issue: 1	Date: 25.04.14

6. References

Alsdorf D.E., Rodriguez E., & Lettenmaier D.P. (2007). Measuring surface water from space. *Reviews of Geophysics*, 45, DOI: 10.1029/2006RG000197.

Andreadis, K.M., Clark, E.A., Lettenmaier, D.P., & Alsdorf, D.E., (2007). Prospects for river discharge and depth estimation through assimilation of swath-altimetry into a raster-based hydrodynamics model, *Geophysical Research Letters*, 34, L10403, doi:10.1029/2007GL029721

Barbetta, S., & Moramarco, T. (2014). Real-time flood forecasting by relating local stage and remote discharge. *Hydrological Sciences Journal*, (accepted).

Baup, F., Frappart, F., & Maubant, J. (2013) Combining high-resolution satellite images and altimetry to estimate the volume of small lakes, *Hydrol. Earth Syst. Sci. Discuss.*, 10, 15731-15770, doi:10.5194/hessd-10-15731-2013.

Bent, R.B., Llewellyn, S.K. & Schmid, P.E. (1972) A Highly Successful Empirical Model for the Worldwide Ionospheric Electron Density Profile, DBA Systems, Melbourne, Florida.



Berry, P. A. M., Garlick, J. D., Freeman, J. A., & Mathers, E. L. (2005). Global inland water monitoring from multi-mission altimetry. *Geophysical Research Letters*, 32, DOI: 10.1029/2005GL022814

Berry, P.A.M., Freeman, J.A., Rogers, C., & Benveniste, J., (2007) Global analysis of Envisat RA-2 burst mode echo sequences. *IEEE Geoscience and Remote Sensing*, 4, 2869-2874 DOI: 10.1109/TGRS.2007.902280.

Berry, P.A.M., Wheeler, J., & Smith, R.G., (2009a). Inland Water Monitoring from Multi-mission Satellite Radar Altimetry - Current Status and Future capability. *The Proceedings of the Earth Observation and Water Cycle Science; 18th-20th November, ESA ESRIN, Frascati, Italy; ISBN 978-92-9221-238-4.*

Berry, P.A.M., Smith, R.G., & Witheridge, S.(2009b) The Global Characterization of Inland Surface Water Observed with the EnviSat Individual Echoes. *The Proceedings of the Earth Observation and Water Cycle Science; 18th-20th November, ESA ESRIN, Frascati, Italy; ISBN 978-92-9221-238-4*

Berry, P.A.M., Smith, R.G., Witheridge, S. & Wheeler, J., (2010a). Global Inland water monitoring from Satellite Radar Altimetry - a glimpse into the future. *Proceedings of the ESA Living Planet Symposium, Bergen, Norway, 27th June - 2nd July.*

		ESA Contract:	1/6287/11/I-NB
		Doc. No:	D2100 Preliminary Analysis Report –draft
		Issue: 1	Date: 25.04.14

Berry, P. A. M., Smith R. G. & Benveniste J., (2010b). ACE2: The New Global Digital Elevation Model, , Gravity, Geoid and Earth Observation International Association of Geodesy Symposia, Volume 135, Part 3, 231-237, 2010

Berry, P. A., Smith, R. G., Salloway, M. K., & Benveniste, J. (2012). Global Analysis of EnviSat Burst Echoes Over Inland Water. *Geoscience and Remote Sensing, IEEE Transactions on*, 50, 1980-1985.

Biancamaria, S., Durand, M., Andreadis, K.M., Bates, P., Boone, A., Mognard, N., Rodriguez, E., Alsdorf, D., Lettenmaier, D.P. & Clark, E.A. (2011). Assimilation of virtual wide swath altimetry to improve Arctic river modeling. *Remote Sensing of Environment*, 115(2), 373-381.

Bilitza, D. & Reinisch, B. (2008) International Reference Ionosphere 2007: Improvements and new parameters, *J. Adv. Space Res.*, 42, 599-609, doi:10.1016/j.asr.2007.07.048.

Birkett, C. M., Mertes, L. A. K., Dunne, T., Costa, M. H., & Jasinski, M. J. (2002). Surface water dynamics in the Amazon Basin: Application of satellite radar altimetry. *Journal of Geophysical Research: Atmospheres* , 107(D20), 8059-8080.

Birkinshaw, S.J., O'Donnell, G.M., Moore, P., Kilsby, C.G., Fowler, H.J. & Berry, P.A.M., (2010). Using satellite altimetry data to augment flow estimation techniques on the Mekong River. *Hydrological Processes*, 24, 3811-3825



Birkinshaw, S. J., Moore, P., Kilsby, C. G., O'Donnell, G. M., Hardy, A. J., & Berry, P. A. M. (2014). Daily discharge estimation at ungauged river sites using remote sensing. *Hydrological Processes*, 28, 1043-1054.

Bjerklie, D.M., Dingman, S.L., Vorosmarty, C.J., Bolster, C.H. & Congalton, R.G., (2003). Evaluating the potential for measuring river discharge from space. *Journal of Hydrology*, 278, 17-38.

Bjerklie, D.M., Moller, D., Smith, L.C. & Dingman, S.L., (2005). Estimating discharge in rivers using remotely sensed hydraulic information. *Journal of Hydrology*, 309, 191-209.

Boy, F., Desjonquères, J.-D., Picot, N., Moreau, T., Labroue, S., Poisson, J.-C. & Thibaut, P., (2012). CryoSat processing prototype: LRM and SAR processing on CNES side, In *Proceedings of the Ocean Surface Topography Science Team Meeting, Venice-Lido*.

Brakenridge, G. R., Nghiem, S. V., Anderson, E., & Mic, R. (2007). Orbital microwave measurement of river discharge and ice status. *Water Resources Research*, 43(4), DOI: 10.1029/2006WR005238.

		ESA Contract:	1/6287/11/I-NB
		Doc. No:	D2100 Preliminary Analysis Report –draft
		Issue: 1	Date: 25.04.14

Brakenridge, R. G., Cohen, S., Kettner, A. J., De Groeve, T., Nghiem, S. V., Syvitski, J. P., & Fekete, B. M. (2012). Calibration of satellite measurements of river discharge using a global hydrology model. *Journal of Hydrology*, 475, 123-136.

Brown, G. S. (1977). The average impulse response of a rough surface and its applications. *Antennas and Propagation, IEEE Transactions on*, 25, 67-74.

Calmant, S., da Silva, J. S., Moreira, D. M., Seyler, F., Shum, C. K., Crétaux, J. F., & Gabalda, G. (2013). Detection of Envisat RA2/ICE retracked radar altimetry bias over the Amazon basin rivers using GPS. *Advances in Space Research*, 51, 1551-1564.

Cauhop´e M., Gennero M.C., DoMinh K., Cretaux J.F., Berge-Nguyen M., Cazenave A., Seyler F. (2006). Worldwide validation of satellite altimetry-based water level time series. EGU06-A-02342, HS52, EGU General Assembly 2006, 02–07 April 2006 Wien (Austria).

Chang, H. C., Li, X., & Ge, L. (2010). Assessment of SRTM, ACE2 and ASTER-GDEM using RTK-GPS. In: AUSTRALASIAN REMOTE SENSING & PHOTOGRAMMETRY CONFERENCE, 15, 2010. University of New South Wales, Sydney, Australia, , p. 13-17.

Chow, V. T., Maidment, D. R., & Mays, L. W. (1988). *Applied hydrology*. McGraw-Hill Series in Water Resources and Environmental Engineering. McGraw-Hill: New York. ISBN 0-07-010810-2. xiii, 572 pp.



Cipollini, P., West, L., Gommenginger, C., Snaith, H., Benveniste, J., Dinardo, S., Donlon, C. (2013) Coastal SAR altimetry data from the eSurge processor , Cryosat 3rd User Workshop, 2013, Dresden.

Coe, M.T.(2000). Modeling terrestrial hydrological systems at the continental scale: Testing the accuracy of an atmospheric GCM. *Journal of Climate*, 13, 686-704.

Coe, M. T., & Birkett, C. M. (2004). Calculation of river discharge and prediction of lake height from satellite radar altimetry: Example for the Lake Chad basin. *Water Resources Research*, 40, W10205, DOI: 10.1029/2003WR002543.

Cotton, P.D., Andersen O., Berry, P., Cipollini, P., Gommenginger, G., Martin-Puig, C., Stenseng, L., Benveniste, J., & Dinardo, S., (2010). The SAMOSA Project: Assessing the Potential Improvements offered by SAR Altimetry Over the Open Ocean, Coastal Waters, Rivers and Lakes., ESA Living Planet Symposium, Bergen, Norway, 27th June - 2nd July

Cotton, P.D. et al., (2013). CP40 CryoSat Plus for Oceans ESA/ESRIN Contract No. 4000106169/12/I-NB D2.1 Preliminary Analysis Report (PAR)

		ESA Contract:	1/6287/11/I-NB
		Doc. No:	D2100 Preliminary Analysis Report –draft
		Issue: 1	Date: 25.04.14

Crétaux, J. F., Jelinski, W., Calmant, S., Kouraev, A., Vuglinski, V., Bergé-Nguyen, M., & Maisongrande, P. (2011). SOLS: A lake database to monitor in the Near Real Time water level and storage variations from remote sensing data. *Advances in Space Research*, 47, 1497-1507.

Crétaux, J. F., Berge-Nguyen, M., Calmant, S., Romanovski, V. V., Meyssignac, B., Perosanz, F., & Maisongrande, P. (2013). Calibration of Envisat radar altimeter over Lake Issykkul. *Advances in Space Research*, 51, 1523-1541.

Dinardo, S. (2013) Guidelines for the SAR (Delay-Doppler) L1b processing, Tect. Note., ESA

Dibarboure, G., Renaudie, C., Pujol, M. I., Labroue, S., & Picot, N. (2012). A demonstration of the potential of Cryosat-2 to contribute to mesoscale observation. *Advances in Space Research*, 50, 1046-1061.

Dibarboure, G., Le Traon, P. Y., & Galin, N. (2013). Exploring the Benefits of Using CryoSat-2's Cross-Track Interferometry to Improve the Resolution of Multisatellite Mesoscale Fields. *Journal of Atmospheric & Oceanic Technology*, 30, 1511-1526.

Duan, Z., & Bastiaanssen, W. G. M. (2013). Estimating water volume variations in lakes and reservoirs from four operational satellite altimetry databases and satellite imagery data. *Remote Sensing of Environment*, 134, 403-416.

Durand, M., Andreadis, K. M., Alsdorf, D. E., Lettenmaier, D. P., Moller, D., & Wilson, M. (2008). Estimation of bathymetric depth and slope from data assimilation of swath altimetry into a hydrodynamic model. *Geophys. Res. Lett.*, 35, DOI: 10.1029/2008GL034150.



ESA (2007). European Space Agency ,CryoSat Mission and Data Description, (http://esamultimedia.esa.int/docs/Cryosat/Mission_and_Data_Descrip.pdf)

ESA (2013). European Space Agency, CryoSat Mission online resources. Available at: <https://earth.esa.int/web/guest/missions/esa-operational-eo-missions/cryosat10.1093/gji/ggt469>.

ESRIN (2013). European Space Research Institute (ESRIN) – European Space Agency and Mullard Space Science Laboratory – University College London. CryoSat Product Handbook. Available at: <https://earth.esa.int/web/guest/missions/esa-operational-eo-missions/cryosat10.1093/gji/ggt469.html>

Fernandes, M.J., Nunes, A.L. & Lázaro, C. (2013) Analysis and Inter-Calibration of Wet Path Delay Datasets to Compute the Wet Tropospheric Correction for CryoSat-2 over Ocean. *Remote Sens.*, 5, 4977-5005.

Fekete, B.M., & Vorosmarty, C.J., (2007). The current status of global river discharge monitoring and potential new technologies complementing traditional discharge measurements,

		ESA Contract:	1/6287/11/I-NB
		Doc. No:	D2100 Preliminary Analysis Report –draft
		Issue: 1	Date: 25.04.14

Predictions in Ungauged Basins: PUB Kick-off (Proceedings of the PUB Kick-off meeting held in Brasilia, 20–22 November 2002), IAHS Publ. 309, Brasilia, 129-136.

Förste, C., Bruinsma, S., Shako, R., Marty, J. C., Flechtner, F., Abrikosov, O., & Balmino, G (2011). EIGEN-6: A new combined global gravity field model including GOCE data from the collaboration of GFZ-Potsdam and GRGS Toulouse, EGU.

Frappart F., Calmant S., Cauhopé M., Seyler F., & Cazenave A. (2006a). Preliminary results of ENVISAT RA-2 derived water levels validation over the Amazon basin. *Remote Sens. Environ.* 100, 252–264.

Frappart F., Do Minh K., L’Hermitte J., Cazenave A., Ramillien G., Le Toan T., & Mognard-Campbell N. (2006b). Water volume change in the lower Mekong from satellite altimetry and imagery data. *Geophys. J. Int.* 167, 570–584.

Galín, N., Wingham, D. J., Cullen, R., Fornari, M., Smith, W. H., & Abdalla, S. (2013). Calibration of the CryoSat-2 interferometer and measurement of across-track ocean slope. *Geoscience and Remote Sensing, IEEE Transactions on*, 51, 57-72.

Gao, H., Birkett, C., Lettenmaier, D.P., (2012). Global monitoring of large reservoir storage from satellite remote sensing, *Water Resources Research*, 48, DOI: 10.1029/2012WR012063.

Garcia, E. S., Sandwell, D. T., & Smith, W. H. (2014). Retracking CryoSat-2, Envisat and Jason-1 radar altimetry waveforms for improved gravity field recovery. *Geophysical Journal International*, doi: 10.1093/gji/ggt469



Getirana, A.C.V., (2010). Integrating spatial altimetry data into the automatic calibration of hydrological models, *Journal of Hydrology*, 387(3-4), 244-255.

Gleason, C. J., & Smith, L. C. (2014). Toward global mapping of river discharge using satellite images and at-many-stations hydraulic geometry. *Proceedings of the National Academy of Sciences*, 201317606.

Gommenginger, C., Martin-Puig, C., Dinardo, S., Raney R.K., Cipollini, P., Cotton, D. and Benveniste, J., (2011). On the performance of CryoSat-2 SAR mode over water surfaces. In *Proceedings of the ESA CryoSat Validation Workshop*, Frascati, Italy.

Gommenginger, C., Martin-Puig, C., Srokosz, M., Caparrini, M., Dinardo, S., and Lucas, B., (2012) Detailed Processing Model of the Sentinel-3 SRAL SAR altimeter ocean waveform retracker, SAMOSA3 WP2300 technical Note, ESRIN Contract No. 20698/07/I-LG "Development of SAR Altimetry Mode Studies and Applications over Ocean, Coastal Zones and Inland Water", Version 2.1.0, 16 March 2012, 75 pages.

GRDC. (2011). The Global Runoff Data Centre, 56068

		ESA Contract:	1/6287/11/I-NB
		Doc. No:	D2100 Preliminary Analysis Report –draft
		Issue: 1	Date: 25.04.14

Hirt C. & M. Kuhn, M. (2012). Evaluation of high-degree series expansions of the topographic potential to higher-order powers, *JGR Solid Earth* doi:10.1029/2012JB009492

Hirt, C., Kuhn, M., Featherstone, W.E., & Goettl, F. (2012) Topographic/isostatic evaluation of new-generation GOCE gravity field models, *Journal of Geophysical Research - Solid Earth*. B05407, doi: 10.1029/2011JB008878

Hydroweb (2011). http://www.legos.obs-mip.fr/soa/hydrologie/hydroweb/Page_2.html

Khajeh, S., Jazireeyan, I., & Ardalan, A. A. (2013). Applying Satellite Altimetry to Wetland Water Levels Monitoring (Case Study: Louisiana Wetland). *Geoscience and Remote Sensing Letters, IEEE*, 11, 1475 - 1478 doi: 10.1109/LGRS.2013.2295831

Kouraev A.V., Zakharova E.A., Samain O., Mognard N.M., Cazenave A. (2004). Ob' river discharge from TOPEX/Poseidon satellite altimetry (1992-2002). *Remote Sensing of Environment*, 93, 238-245.

Kouraev, A.V., Shimaraev, M.N., Buharizin, P.I., Naumenko, M.A., Cretaux, J. F., Mognard, N., Legresy, B., Remy, F. (2008) Ice and Snow Cover of Continental Water Bodies from Simultaneous Radar Altimetry and Radiometry Observation. *Surveys in Geophysics*, 29, 271–295
<http://dx.doi.org/10.1007/s10712-008-9042-2>



Kouraev, A.V., Kostianoy, A.G., Lebedev, S.A. (2009) Ice cover and sea level of the Aral Sea from satellite altimetry and radiometry (1992–2006). *Journal of Marine Systems*, 76, 272–286
<http://dx.doi.org/10.1016/j.jmarsys.2008.03.016>

Leon J.G., Calmant, S., Seyler, F., Bonnet, M.P., Cauhope, M., Frappart, F., Filizola, N., & Fraizy, P. (2006). Rating curves and estimation of average water depth at the upper Negro River based on satellite altimeter data and modeled discharges. *Journal of Hydrology*, 328, 481-496.

Li, Z. Muller, J.P., Cross, P., Albert, P., Fischer, J. & Bennartz, R. (2006) Assessment of the potential of MERIS near-infrared water vapour products to correct ASAR interferometric measurements. *International Journal of Remote Sensing*, 27, 349-365.

Li, Z., Fielding, E.J., Cross, P. & Preusker, R., (2009). Advanced InSAR atmospheric correction: MERIS/MODIS combination and stacked water vapour models, *International Journal of Remote Sensing* 30, 3343-3363.

Longuevergne, L., Wilson, C. R., Scanlon, B. R., & Crétaux, J. F. (2013). GRACE water storage estimates for the Middle East and other regions with significant reservoir and lake storage. *Hydrol. Earth Syst. Sci.*, 17, 4817–4830.

		ESA Contract:	1/6287/11/I-NB
		Doc. No:	D2100 Preliminary Analysis Report –draft
		Issue: 1	Date: 25.04.14

Maheu, C., Cazenave, A., & Mechoso, C. R. (2003). Water level fluctuations in the Plata basin (South America) from Topex/Poseidon satellite altimetry. *Geophysical research letters*, 30, DOI: 10.1029/2002GL016033.

METI & NASA (2011). ASTER <http://www.ersdac.or.jp/GDEM/E/1.html>

Michailovsky, C. I., McEnnis, S., Berry, P. A. M., Smith, R. & Bauer-Gottwein, P. (2012). River monitoring from satellite radar altimetry in the Zambezi River Basin. *Hydrology and Earth System Sciences*, 16, 2181-2192

Michailovsky, C.I., & Bauer-Gottwein, P., (2014). Operational reservoir inflow forecasting with radar altimetry: The Zambezi case study, *Hydrology and Earth System Sciences*, 18, 997-1007.

Michailovsky, C.I., Milzow, C., & Bauer-Gottwein, P., (2013). Assimilation of radar altimetry to a routing model of the Brahmaputra River, *Water Resources Research*, 49, 4807–4816.

Milzow, C., Krogh, P.E. & Bauer-Gottwein, P. (2011). Combining satellite radar altimetry, SAR surface soil moisture and GRACE total storage changes for model calibration and validation in a large ungauged catchment. *Hydrology and Earth System Sciences*, 15, 1729-1743

Moore, P. & Williams S.D.P (2014) Integration of Altimetric Lake Levels and GRACE Gravimetry over Africa: Inferences for Groundwater Change 2003-2011. *Water Resources Research* (submitted)

Muste, M., Yu, K., & Spasojevic, M.,(2004). Practical aspects of ADCP data use for quantification of mean river flow characteristics; Part 1: moving-vessel measurements, *Flow Measurement and Instrumentation*, 15, 1-16.



NASA JPL, 2011, <http://www2.jpl.nasa.gov/srtm/>

Nijssen, B., O'Donnell, G.M., Lettenmaier, D.P., Lohmann, D. & Wood, E.F. (2001). Predicting the discharge of global rivers. *Journal of Climate*, 14, 3307-3323.

Papa, F., Durand, F., Rossow, W.B., Rahman, A., Bala, S.K., (2010). Satellite altimeter-derived monthly discharge of the Ganga-Brahmaputra River and its seasonal to interannual variations from 1993 to 2008. *Journal of Geophysical Research-Oceans*, 115, DOI: 10.1029/2009JC006075.

Pavlis, N.K., Holmes, S.A., Kenyon, S.C. & Factor, J.K. , (2012) The development and evaluation of the Earth Gravitational Model 2008 (EGM2008) *JGR: Solid Earth Volume*, 117, B4.

Pereira-Cardenal, S.J., Riegels, N.D., Berry, P.A.M., Smith, R.G., Yakovlev, A., Siegfried, T.U. & Bauer-Gottwein, P. (2011). Real-time remote sensing driven river basin modelling using radar altimetry. *Hydrology and Earth System Sciences*, 15, 241-254

		ESA Contract:	1/6287/11/I-NB
		Doc. No:	D2100 Preliminary Analysis Report –draft
		Issue: 1	Date: 25.04.14

Pfeffer, J., Seyler, F., Bonnet, M. P., Calmant, S., Frappart, F., Papa, F., & Santos Da Silva, J. (2014). Low-water maps of the groundwater table in the central Amazon by satellite altimetry. *Geophysical Research Letters*. DOI: 10.1002/2013GL059134

Qian, T.T., Dai, A., Trenberth, K.E., Oleson, K.W., (2006). Simulation of global land surface conditions from 1948 to 2004. Part I: Forcing data and evaluations. *Journal of Hydrometeorology*, 7, 953-975.

Raney, R. K. (1998). The delay/Doppler radar altimeter, *IEEE Trans. Geosci. Remote Sens.*, 36, 1578 – 1588.

Ray, C., Martin-Puig, C., Clarizia, M.P., Ruffini, G., Dinardo, S., Gommenginger C. and Benveniste, J. (2013) SAR altimeter backscattered waveform model. Submitted to *IEEE Trans. On Geoscience and Remote Sensing*.

Ricko, M., Birkett, C.M., Carton, J.A., & Cretaux, J.-F. (2012) Intercomparison and validation of continental water level products derived from satellite radar altimetry, *Journal of Applied Remote Sensing*, 6.

Salstein, D. A., Ponte, R. M., & Cady-Pereira, K. (2008) Uncertainties in atmospheric surface pressure fields from global analyses, *J. Geophys. Res.*, 113, D14107, doi:10.1029/2007JD009531.



Salvia, M., Grings, F., Barraza, V., Perna, P., Karszenbaum, H., & Feirazzoli, P. (2012). Active and passive microwave systems in the assessment of flooded area fraction and mean water level in the Paraná River floodplain. In *Microwave Radiometry and Remote Sensing of the Environment (MicroRad)*, 2012 12th Specialist Meeting on (pp. 1-4). IEEE.

Santos da Silva, J., Seyler, F., Calmant, S., Corrêa Rotuno Filho, O., Roux, E., Magalhaes, A. A., & Guyot, J.-L. (2012) Water level dynamics of Amazon wetlands at the watershed scale by satellite altimetry, *Int. J. Remote Sens.*, 33, 200–206.

Schrama, E., et al., (2013). CryoSat-2 Precision Orbit Determination Including Altimeter Calibration and Validation, *Cryosat 3rd User Workshop*, March 2013, Dresden

Scharroo, R., Smith, W.H.F., & Lillibridge, J., (2008). A new GPS-based climatology for the total electron content in the ionosphere. *OSTST Meeting 2008*, Nice, France.

Shako, R., Förste, C., Abrikosov, O., Bruinsma, S., Marty, J. C., Lemoine, J. M., & Dahle, C. (2014). EIGEN-6C: A high-resolution global gravity combination model including GOCE data. In *Observation of the System Earth from Space-CHAMP, GRACE, GOCE and future missions* (pp. 155-161). Springer Berlin Heidelberg.

		ESA Contract:	1/6287/11/I-NB
		Doc. No:	D2100 Preliminary Analysis Report –draft
		Issue: 1	Date: 25.04.14

Smith R.G. & Berry, P.A.M., (2011). Evaluation of the differences between the SRTM and Satellite Radar Altimetry height measurements and the approach taken for the ACE2 GDEM in areas of large disagreement, *Journal of Environmental Monitoring*, 2011, 13, 1646 – 1652

Smith, L.C., & Pavelsky, T.M., (2009). Remote sensing of volumetric storage changes in lakes, *Earth Surface Processes and Landforms*, 34, 1353-1358.

Stenseng, L., & Andersen, O. B. (2012). Preliminary gravity recovery from CryoSat-2 data in the Baffin Bay. *Advances in Space Research*, 50, 1158-1163.

Tang Q., Gao H., Lu H., Lettenmaier D.P. (2009). Remote sensing: hydrology. *Progress in Physical Geography*, 33, 490-509.

Tarpanelli, A., Barbetta, S., Brocca, L., & Moramarco, T. (2013). River Discharge Estimation by Using Altimetry Data and Simplified Flood Routing Modeling. *Remote Sensing*, 5, 4145-4162.

Temimi, M., Leconte, R., Brissette, F., & Chaouch, N. (2007). Flood and soil wetness monitoring over the Mackenzie River Basin using AMSR-E 37GHz brightness temperature. *Journal of Hydrology*, 333, 317-328.

Temimi, M., Lacava, T., Lakhankar, T., Tramutoli, V., Ghedira, H., Ata, R., & Khanbilvardi, R. (2011). A multi-temporal analysis of AMSR-E data for flood and discharge monitoring during the 2008 flood in Iowa. *Hydrological Processes*, 25, 2623-2634.

USDA(2011). http://www.pecad.fas.usda.gov/cropexplorer/global_reservoir/



Van Dijk, A. I. J. M., Renzullo, L. J., Wada, Y., and Tregoning, P. (2013) A global water cycle reanalysis (2003–2012) reconciling satellite gravimetry and altimetry observations with a hydrological model ensemble, *Hydrol. Earth Syst. Sci. Discuss.*, 10, 15475-15523, doi:10.5194/hessd-10-15475-2013.

Vörösmarty, C. J., McIntyre, P. B., Gessner, M. O., Dudgeon, D., Prusevich, A., Green, P., & Davies, P. M. (2010). Global threats to human water security and river biodiversity. *Nature*, 467, 555-561.

Ward, P.J., Aerts, J., de Moel, H., Renssen, H., (2007). Verification of a coupled climate-hydrological model against Holocene palaeohydrological records. *Global and Planetary Change*, 57, 283-300.

Werth, S., Guntner, A., (2010). Calibration analysis for water storage variability of the global hydrological model WGHM. *Hydrology and Earth System Sciences*, 14, 59-78.

Werth, S., Guntner, A., Petrovic, S., Schmidt, R., (2009). Integration of GRACE mass variations into a global hydrological model. *Earth and Planetary Science Letters*, 277, 166-173.

		ESA Contract:	1/6287/11/I-NB
		Doc. No:	D2100 Preliminary Analysis Report –draft
		Issue: 1	Date: 25.04.14

Wheeler, J., Berry, P.A.M., Smith, R.G., & Benveniste, J., (2010). The ESA Near-Real-Time River & Lake Processor. ESA Living Planet Symposium, Bergen, Norway, 27th June - 2nd July.

Wingham, D. J., Francis, et al., (2006). CryoSat: A mission to determine the fluctuations in Earth's land and marine ice fields. *Advances in Space Research*, 37 (4), 841-871.
doi:10.1016/j.asr.2005.07.027

Wingham, D. J., L. Phalippou, C. Mavrocordatos, & D. Wallis (2004), The mean echo and echo cross product from a beamforming interferometric altimeter and their application to elevation measurement. *IEEE Trans. Geosci. Remote Sens.*, 42, 2305 – 2323.

Witheridge, S., Berry, P.A.M., & Smith, R.G. (2010) Analysis of EnviSat RA-2 Burst Echoes over Lake surfaces. *Proceedings of the ESA Living Planet Symposium, Bergen, Norway, 27th June - 2nd July.*

Yamazaki, D., Kanae, S., Kim, H., Oki, T., (2011). A physically based description of floodplain inundation dynamics in a global river routing model, *Water Resources Research*, 47, DOI: 10.1029/2010WR009726.

Yamazaki, D., Lee, H., Alsdorf, D.E., Dutra, E., Kim, H., Kanae, S., Oki, T., (2012). Analysis of the water level dynamics simulated by a global river model: A case study in the Amazon River, *Water Resources Research*, 48, DOI: 10.1029/2012WR011869.



Zakharova, E.A., Kouraev, A.V., Cazenave, A., Seyler, F. (2006). Amazon River discharge estimated from TOPEX/Poseidon altimetry. *Comptes Rendus Geoscience*, 338, 188-196.

Zakharova, E.A., Kouraev, A.V., Kolmakova, M.V., Mognard, N.M., Zemtsov, V.A., Kirpotin, S.N., (2009). The modern hydrological regime of North-Western Siberia from in situ and satellite observations. *Int J Environ Studies*, 66, 447–463, doi: 10.1080/00207230902823578.

Zakharova, E.A., Kouraev, A.V., Biancamaria, S., Kolmakova, M.V., Mognard, N.M., Zemtsov, V.A., Kirpotin, S.N., Decharme, B. (2011) Snow Cover and Spring Flood Flow in the Northern Part of Western Siberia (the Poluy, Nadym, Pur, and Taz Rivers) *Journal of Hydrometeorology*, 12, 1498–1511 <http://dx.doi.org/10.1175/JHM-D-11-017.1>

Zakharova, E. A., Kouraev, A. V., Rémy, F., Zemtsov, V. A., & Kirpotin, S. N. (2014). Seasonal variability of the Western Siberia wetlands from satellite radar altimetry. *Journal of Hydrology*. <http://dx.doi.org/10.1016/j.jhydrol.2014.03.002>

Zandbergen, P. (2008). Applications of shuttle radar topography mission elevation data. *Geography Compass*, 2, 1404-1431.

		ESA Contract:	1/6287/11/I-NB
		Doc. No:	D2100 Preliminary Analysis Report –draft
		Issue: 1	Date: 25.04.14

Zhang, Y., Hong, Y., Gourley, J.J., Wang, X., Brakenridge, G.R., and De Groeve, T., (2014). Impact of assimilating spaceborne microwave signals for improving hydrological prediction in ungauged basins. American Geophysical Union Monograph. (in press)